Crustal shortening at the Sierra Pie de Palo (Sierras Pampeanas, Argentina): near-surface basement folding and thrusting

Nicolas Bellahsen, Michel Sébrier, Lionel Siame

Crustal shortening at the Sierra Pie de Palo (Sierras Pampeanas, Argentina): near-surface basement folding and thrusting

N. Bellahsen[1*], M. Sebrier[1], L. Siame[2]

[1] Sorbonne Universités, UPMC Univ Paris 06, CNRS, Institut des Sciences de la Terre de Paris (iSTeP), 4 place Jussieu 75005 Paris, France
[2] Aix-Marseille Université, CNRS-IRD-Collège de France, UM34 Centre Européen de Recherche et d'Enseignement des Géosciences l'Environnement, Technopôle de l'Arbois, Aix-en-Provence, France

* Corresponding author: nicolas.bellahsen@upmc.fr

Abstract
The Sierra Pampeanas consist of basement uplifts that are mainly controlled by W-verging crustal thrusts. One of them, the Sierra Pie de Palo, is controlled by a blind thrust whose kinematics is debated. We analyzed the reverse faults located along the eastern side of the range and show that these are characterized by small displacements (few hundreds of meters) of the Neogene and Quaternary deposits controlled by the inherited basement metamorphic foliation and shear zones. At the sierra scale, the inherited foliation pattern appears already folded, before the Cenozoic shortening, forming a series of antiforms and synforms with various wavelengths. We propose that this structure is amplified during the Plio-Quaternary shortening resulting in a large asymmetrical basement-cored anticline where foliation-parallel slip can act as folding mechanism. The overall kinematics is consistent with an E-verging fault-propagation fold; this proposed kinematics is an alternative to the frequently suggested W-verging fault-bend fold model. Finally, we propose a new, alternative, and speculative crustal and lithospheric structure for this region consisting in two E-verging basement thrusts coeval to W-verging Pampean thrusts, both rooting below the Precordillera, above an eclogitized lower crust.

Crustal shortening at the Sierra Pie de Palo (Sierras Pampeanas, Argentina): near-surface basement folding and thrusting

Abstract

The Sierra Pampeanas consist of basement uplifts that are mainly controlled by W-verging crustal thrusts. One of them, the Sierra Pie de Palo, is controlled by a blind thrust whose kinematics is debated. We analyzed the reverse faults located along the eastern side of the range and show that these are characterized by small displacements (few hundreds of meters) of the Neogene and Quaternary deposits controlled by the inherited basement metamorphic foliation and shear zones. At the sierra scale, the inherited foliation pattern appears already folded, before the Cenozoic shortening, forming a series of antiforms and synforms with various wavelengths. We propose that this structure is amplified during the Plio-Quaternary shortening resulting in a large asymmetrical basement-cored anticline where foliation-parallel slip can act as folding mechanism. The overall kinematics is consistent with an E-verging fault-propagation fold; this proposed kinematics is an alternative to the frequently suggested W-verging fault-bend fold model. Finally, we propose a new, alternative, and speculative crustal and lithospheric structure for this region consisting in two E-verging basement thrusts coeval to W-verging Pampean thrusts, both rooting below the Precordillera, above an eclogitized lower crust.

1. Introduction

In the upper crust, deformation usually localizes on major faults because of the frictional mechanical behavior and strain weakening active in the crust (e.g., Collettini et al., 2009). A notable exception is the sedimentary cover that has the ability to fold mainly because of the mechanical stratigraphy with weak, low stress interbeds. Thus, in contractional setting, sedimentary cover usually deforms with typical fold and thrust belt kinematics. In the basement, however, mainly composed of crystalline rocks, the deformation is more localized than in the sedimentary cover. Only approaching the brittle-ductile transition, and below, the deformation gets distributed mainly due to temperature increase.

Thus, for basement rocks in the upper crust up to the surface, our understanding of crustal rheology will predict localized, major faults. In some cases, however, the deformation is seen as more distributed in the field. This distributed, though brittle, deformation have been observed at a few places, mainly in the Laramide Orogenic belt (Rocky Mountains), as well as in South America: they are interpreted either as basement deformation over a fault-bend fold (Casas et al., 2003) or in a fault-propagation fold with triangular zones of shear ahead or near the thrust upper tip (Schmidt, Genovese & Chase, 1993; Beaudoin et al., 2012; Erslev, 1991; Bump, 2003; Garcia & Davis, 2004).

The Sierras Pampeanas (**Fig. 1**), a modern analogue of the Laramide Rocky Mountains (Jordan & Allmendinger, 1986), provide a unique setting for studying basement deformation in a shallow brittle setting. The Sierra Pie de Palo (**Fig. 1, 2, 3**) is a basement uplift in the Sierras Pampeanas, NW Argentina. It is topped by a 3000m-high perched erosional surface that attests for a significant structural relief. This structure is interpreted either as a fault-bend fold on a W-verging thrust (Ramos, Cristallini & Pérez, 2002; Vergés et al., 2007) or as a fold above an E-verging blind thrust that branches at depth on a W-verging thrust (Siame, Bellier & Sebrier, 2006; Siame et al., 2002; Siame et al., 2015). In both cases, these models imply some distributed deformation in the basement that necessitates a detailed study.

Thanks to excellent outcrop conditions in the Pie de Palo area, we combined structural and microstructural observations along its eastern margin and available data to propose a model for basement folding integrating outcrop- and crustal-scale interpretations. In particular, we propose that, in the uppermost crust, the shortening, localized on inherited foliation planes that folded and evolved as cataclastic faults, may have allowed folding of the upper crust above a E-verging blind thrust. We propose new cross-sections at crustal- and lithospheric-scale that are consistent with the geological and geophysical data and constitute an alternative model for Andean shortening in the specific Andean backarc province (Cuyania crust).

2. Regional setting of the Sierras Pampeanas.

The Pie de Palo anticline is one of the Sierras Pampeanas ranges that extends between latitudes 27° and 33° S and longitudes 64 and 68° W (**Fig. 1b**). These ~N-striking ranges (NNW to NNE) correspond to Neogene-Quaternary basement-block uplifts, which are located to the East of the Andes (**Fig. 1**). These basement blocks extend where the Nazca slab, which is subducting eastward below the western edge of the South American plate, flattens below the Andes at a depth of ~100 km (Jordan et al., 1983; Jordan & Allmendinger, 1986; Cahill & Isacks, 1992; Ramos, Cristallini & Pérez, 2002; Anderson et al., 2007). This segment of the Andean subduction is characterized by a ~N75°E-trending convergence with a rate of about 75 mm/yr (DeMets et al., 1990). The flat slab geometry appears to result from the subduction of the Juan Fernandez aseismic ridge **(Fig. 1a)**, which increases the buoyancy of the Nazca plate (Pilger, 1981; Gutscher et al., 2000). This ridge subduction initiated between 14 Ma and 11 Ma, moving from north to south along the Chilean trench (Yanez et al., 2001). The volcanic arc migrated eastward from ~11 Ma to ~8 Ma to shut off totally by 5 Ma (Kay & Mpodozis, 2002), and the flat geometry reached the retroarc region between Late Miocene and Pliocene (Kay & Abbruzzi, 1996). Indeed, Andean regions with flat slab subduction (e.g. Central Peru and Sierras Pampeanas) are commonly characterized by an extinct volcanic arc and display a much wider shortening retroarc belt because it should accommodate larger amounts of shortening than the neighboring regions characterized by steeper slabs (Jordan et al., 1983; Sébrier et al., 1988). This shortening deformation might also be possibly enhanced by thermal weakness of the crust associated with the eastward migration of the asthenospheric wedge (Ramos, Cristallini & Pérez, 2002).

The 27-33°S retroarc shortening province associated with the Andean flat slab segment comprises two main parts **(Fig. 1b)**: (1) a ~40-km narrow, E-verging, thin-skinned, fold and thrust belt composed of Paleozoic-Mesozoic rocks and extending to the East of the main high Andes from Sierra de Las Planchadas (27.5°S) up to the southern Precordillera in the Mendoza area (33°S) and (2) a ~350-km wide subprovince of mostly W-verging block uplifts made of Precambrian and early Paleozoic metamorphic rocks, i.e., the Sierras Pampeanas. Overall, the E-verging thin-skinned thrusts initiated earlier (Early to Mid Miocene) than the Pampean basement uplifts, which started between the Late Miocene in the northern Sierras Pampeanas and the Pliocene-Quaternary in the southern ones (Jordan et al., 1993; Zapata and Allmendinger, 1996). Indeed, these basements uplifts are located within the distal part of the Miocene foreland basin as out of sequence faulted blocks so that this foreland is generally described as a broken foreland (Jordan et al., 1983). Typically, the sedimentary signature of these uplifts is the onset of conglomerate deposits atop of the previous thin distal sedimentation (Jordan et al., 1993). These blocks uplifts are controlled by the reactivation of inherited crustal weaknesses, such as Proterozoic or Early Paleozoic sutures and Late Paleozoic or Mesozoic graben normal faults (Ramos, Cristallini & Pérez, 2002), which explain their variable lengths from several tens to several hundreds of kilometers. Interestingly, the Pampean ranges have a wide range of altitudes between some ~1000 and 6000 m, with a mean tendency to have higher elevations northward and westward, which may result both from an earlier northern initiation and a larger amount of shortening closer to the Andes.

The area of interest is located on the ~400-km wide south-central profile of the Sierras Pampeanas (~31.5°S), which extends approximately between the cities of San Juan and Cordoba (**Fig. 1b**). Adding the ~50-km wide, thin-skinned fold and thrust belt yields a width of ~450 km for the Neogene to present retroarc shortening province. This central profile offers the following characteristics: (1) it is located just above the central part of the flat slab segment (Anderson et al., 2007), (2) it has been the focus of many geological studies (Ramos, Cristallini & Pérez, 2002 and references herein), particularly in its western stretch where most of the shortening is accommodated, (3) the Neogene to present history of shortening is relatively well constrained to 90 km yielding a regional mean rate of 4.5 mm/yr during the last 20 Ma (Allmendinger et al., 1990; Jordan, Schlunegger & Cardozo, 2001), and (4) the level of crustal seismicity is the highest along this profile in the whole retroarc belt (Smalley et al., 1993; Siame et al., 2005). Consequently, many seismological studies provide information on the crustal seismicity (Kadinsky-Cade & Reilinger, 1985; Regnier et al., 1992; Smalley et al., 1993; Alvarado, Beck & Zandt, 2007; Alvarado et al., 2009; Alvarado et al., 2005; Alvarado & Beck, 2006) and the lithospheric and crustal structures (Ammirati et al., 2015 and references herein). The main results obtained along this profile are summarized hereafter. The eastward cessation of volcanism in the Central Precordillera (68.8°W) by 7 Ma and in the Sierra de Cordoba (65.2°W) by 4.7 Ma (Kay & Abbruzzi, 1996) demonstrates that the flat slab geometry was installed below this profile between the Late Miocene and in the Early Pliocene. The depth of the continental Moho varies along this profile: 66 km below the Central Precordillera (Ammirati et al., 2013), 52 km below the Sierra Pie de Palo (Calkins et al., 2006; Ammirati, Alvarado & Beck, 2015), while it is only 38 km and 35 km below the western and eastern parts of the Sierra de Cordoba, respectively (Perarnau et al., 2012). The highest level of seismicity (Smalley et al., 1993) is located between the Central Precordillera (68.8°W) and the Sierra del Valle Fertil-La Huerta (67.3°W), the base of this crustal seismicity appears deeper than 30 km and might correspond to a ~34-km deep seismic discontinuity, while a shallower one is also observed at a depth of ~18-km (Calkins et al., 2006; Alvarado, Beck & Zandt, 2007; Ammirati, Alvarado & Beck, 2015). This seismic discontinuity near the base of the crustal seismicity could correspond to the main Andean décollement that permits to propagate eastward the Andean shortening to the Sierra Pampeanas. Interestingly, the GPS velocity field measured in this zone of high seismicity suggest a step in their eastward decay that may agree with a shortening rate of ~5 mm/yr (Brooks et al., 2003). Three destructive earthquakes with Mw~7 occurred within this region in 1944, 1952, and 1977. The two older have focal depths of 11 km and 12 km, respectively (Alvarado & Beck, 2006), while the 1977 focus was estimated at ~25-30-km (Alvarado & Beck, 2006 and references herein).

Finally, one important consequence of the slab geometry is the decrease of the thermal gradient in the overlying continental crust. Thermal modeling points a thermal lowering from ~30°C/km (situation above steeper Andean subduction segments) to ~10°/km for the flat segments caused by the lack of asthenospheric wedge (Gutscher et al., 2000). This low thermal gradient has been determined within the sediments of the Neogene basins (Collo et al., 2015) and explains why thermo-chronologic studies have major difficulties constraining the uplift rates of most of the Western Pampean ranges (Davila & Carter, 2013), especially along the central profile of the Sierras Pampeanas (Löbens et al., 2013). Obviously, this also agrees quite well with the uncommon deep crustal seismicity observed in the region (Regnier et al., 1992; Smalley et al., 1993).

3. Geological setting of the Sierra Pie de Palo

The NNE-striking, oval-shaped Sierra Pie de Palo (**Fig. 2, 3**) is located at 31.4°S and 67.9°W. It is 80 km long and 32 km wide, and has an altitude of 3162 m towering above the surrounding 500-600 m elevated desert alluvial plain. This range is bounded by (**Fig. 2**): to the West, the Tulum Valley, a syncline of Neogene and Quaternary beds, which separates the Sierra Pie de Palo from the Eastern Precordillera; to the North stands the 10-km thick Neogene to Quaternary Bermejo foreland basin; to the East, the triangular-shaped, South Bermejo Valley, which is a Neogene to Quaternary synclinorium basin separating the Sierra Pie de Palo from the NNW-striking Sierra Valle Fertil-La Huerta range; to the South, the southern continuation of the Bermejo basin which stands below the Medanos Grandes sand dunes. The first order topography of the Sierra Pie de Palo (**Fig. 3a**) corresponds to a dissymmetric arch with steep eastern and northern slopes whereas the southern and western slopes are gently dipping (Siame et al., 2006; Siame et al., 2015). The western long limb of the range is dissected by two main WSW-striking, rectilinear, deep canyons Guayaupa-Lima and Grande El Molle (**Fig. 3**). However, topographic profiles along the top of the range do not reveal any significant vertical displacement associated with these transverse lineaments. Similarly, they do not displace the rectilinear eastern front of the Pie de Palo range, hence, they should be presently inactive structures (Siame et al., 2015).

The relatively flat areas composing the Sierra Pie de Palo range topography define a convincing surface envelop along both N-S and E-W directions (**Fig. 3**), shaping an anticline fold (Siame et al., 2015). These flat surfaces are actually characteristic of most of the Sierras Pampeanas and have long been referred as the “Pampean peneplain” (Jordan et al., 1989). This “peneplain” appears polygenic as it formed between Middle Paleozoic and Cretaceous (Carignano, Cioccale & Rabassa, 1999; Costa et al., 2000; Rabassa, Carignano & Cioccale, 2010). However, the main debate concerns the timing of its exhumation. Some considered this erosion surface was mostly deformed and exhumed during the Neogene (e.g., Jordan et al., 1989) while others proposed that the Sierras Pampeanas may have been exhumed since the Late Paleozoic or Mesozoic (Carignano, Cioccale & Rabassa, 1999; Rabassa, Carignano & Cioccale, 2010; Löbens et al., 2013; Löbens et al., 2011; Enkelmann et al., 2014). In the Sierra Pie de Palo range, the age of this surface is quite imprecise as it is cutting on basement metamorphic rocks of Early Paleozoic-Proterozoic age (Ramos & Vujovich, 2000) and covered around the range by Neogene continental deposits. These red-beige deposits correspond in the southeastern edge of the Pie de Palo range to the 300-m thick Niquizanga Formation and the overlying 420-m thick Rio del Camperito Formation (Cuerda, Varela & Iniguez, 1983). These two formations are correlated with the Upper Miocene-Lower Pliocene Jachal and Pliocene-Quaternary Mogna Formations, respectively, these are dated in the Bermejo basin to the north of the Pie de Palo range (Jordan et al., 1993; Zapata & Allmendinger, 1996). The Niquizanga Formation, which rests directly upon the “Pampean peneplain”, is composed of thin clastic lacustrine beds containing evaporite facies (halite and gypsum) suggesting that the Neogene topography of the Sierra Pie de Palo range was either very subdued or even almost inexistent at that time so that the “Pampean peneplain” could have been completely covered by the Neogene beds of the

Bermejo foreland basin. The thickness of the Neogene beds might have summed 2-3 km at most (e. g., Ramos & Vujovich, 2000) and more likely 1.9 to 2.4 km (Siame et al., 2015). The first option agrees with a long history of exhumation whereas the second favors a late Cenozoic rapid exhumation. Whatever the initial thickness of Neogene deposits above the "Pampean peneplain", recent cosmogenic nuclide data (^{10}Be) favor a rapid uplift of the Pie de Palo Anticline during the last 2-4 Ma (Siame et al., 2015). Furthermore, the low thermal gradients reported in the Neogene basins (Davila & Carter, 2013; Collo et al., 2015) also indicate that the Pliocene-Quaternary folding and uplift of the metamorphic basement must have occurred under near surface conditions.

The Sierra Pie de Palo range is an actively growing basement anticline associated with a high level of crustal seismicity (Regnier et al., 1992; Smalley et al., 1993; Ramos, Cristallini & Pérez, 2002; Siame, Bellier & Sebrier, 2006; Siame et al., 2015; Siame et al., 2002). This range is bounded by three major faults. The northern boundary of the range corresponds to the North Pie de Palo fault, a ~E-W striking transpressive, left-lateral fault, which extends over 80 km from the Matagusanos basin, south of the Mogna anticline in the Eastern Precordillera (Zapata, 1998) to the Sierra Valle Fértil fault (**Fig. 2**). This regional structure also controls a major northward deepening in the basement depth across the southern boundary of the Bermejo Basin (Jordan & Allmendinger, 1986). It limits the northern edge of the Sierra Pie de Palo along approximately 26 km roughly at the contact between the metamorphic basement and the Neogene and Quaternary deposits. This stretch, which is referred as the Pajaritos Fault (**Fig. 3**) (Costa et al., 2000), displays fairly rectilinear N-facing scarp traces that are quite conspicuous at two locations (31.047°S-67.94°W and 31.057°S -67.84°W). The easternmost location of this Pajaritos Fault affects a series of alluvial fans and exhibits a well-developed 4-km long, north facing fault scarp with a right-stepping relay agreeing with some left-lateral component of slip associated with a steep (45-60°S dipping) reverse movement. This Pajaritos Fault was interpreted as a lateral ramp of the Pie de Palo Anticline and its reverse slip rate determined to ~1 mm/yr (Siame et al., 2015).

The western boundary of the Pie de Palo metamorphic basement with the Tulum Valley syncline is very sinuous and the Quaternary bordering alluvial deposits forms a very poorly incised series of fans. All these landform features suggest that no fault activity is occurring along this western edge of the range. Nevertheless, the south-westernmost contact of the basement with the Tulum Valley displays a topographic step between the “Pampean peneplain” and the valley bottom that might record locally some vertical displacement along the SW Pie de Palo Anticline. Although, this sharper topography might also result from the fluvial erosion of the Precambrian basement by former meanders of the San Juan River, it is located on the possible northern termination of the Tulum fault system (Zambrano & Suvires, 2008) (**Fig. 2**). This fault system, which is not accurately delineated and limits the western edge of the Pampean Precambrian outcrops from the Paleozoic outcrops of the Eastern Precordillera (Ramos, Cristallini & Pérez, 2002), corresponds farther south, at Cerro Salinas, to the emerging ramp of the active Pampean thrust system (Vergés et al., 2007) (**Fig. 2**).

The structure controlling the Pie de Palo range, which strikes N21°E and extends over 65 km, is the most debated as it has been described as dipping E (Langer & Bollinger, 1988; Costa et al., 2000; Ramos, Cristallini & Pérez, 2002) or W (Kadinsky-Cade & Reilinger, 1985; Reilinger & Kadinsky-Cade, 1985). It is noteworthy that, in some interpretations, the E-dipping structure beneath Pie de Palo might root at depth on a W-dipping thrust (Ramos, Cristallini & Pérez, 2002) and in some other, the W-dipping structure branches at depth on a E-dipping thrust (Siame et al., 2015). The E-dipping hypothesis is based on the epicenter location of the 1977 Mw7.4 earthquake within the southern Bermejo Valley, on the observation of W-verging faults affecting the Neogene deposits along the eastern edge of the Sierra Pie de Palo (Ramos, Cristallini & Pérez, 2002), and on the fact that both the Eastern Precordillera and the westernmost Sierras Pampeanas forms a W-verging thrust system. This fault would thus ramp off from the Valle Fértil – La Huerta Fault at a depth of ~30 km. In contrast, the W dipping hypothesis is mainly based on leveling data after the 1977 earthquake showing an uplift of the southern Pie de Palo anticline (Kadinsky-Cade & Reilinger, 1985) and crustal reconstructions from shallow and deep seismic profiling (Zapata, 1998) which favors a W-dipping, E-verging blind fault below the eastern border of the range. This hypothesis is also in good agreement with the observed first-order topographic signature of a steeper eastern flank, with higher Neogene dips along the eastern flank than the western one, and with a higher number of alluvial fans with steeper top surfaces than those that skirt over the western edge (Siame et al., 2015). An intermediate model displays both vergences: In the upper part of the crust the Sierra Pie de Palo is controlled by an E-verging structure that branches at depth on a W-verging one (Siame et al., 2002; 2005; 2015). Moreover, even in the W-verging models, E-verging basement thrusts are also proposed below Pie de Palo (footwall thrust in Verges et al., 2007).

Finally, a temporary seismic network, installed some ten years after the 1977 earthquake, allowed obtaining a much more accurate image of the microseismicity (Regnier et al., 1992) that demonstrated the teleseismic locations are systematically mislocated with an eastward shift of about 30 km. Accounting for this shift, the 1977 epicenter should be moved some 30 km westward, locating the 1977 focus below the southern Pie de Palo range (see discussion). These data also show that the half northern part of the Pie de Palo stands above aligned seismic foci that define on a cross-section a W-dipping fault (**Fig. 4a**), which ramps off from a ~30 km depth and cab be traced upward to a 7 km depth (Regnier et al., 1992). The foci depth distribution in the half southern Pie de Palo provides a less clear image than the northern one, this vertical foci distribution might correspond to a pop-up structure (**Fig. 4b**, see discussion). In summary, the Pie de Palo Anticline has been interpreted either as a fault bend fold (W-verging structure), a fault propagation fold (E-verging structure), or a structure due to the interaction between both E- and W-verging structures. Focusing on puzzling W-verging reverse faults cropping out along the eastern edge and their mechanisms of deformation can help deciphering between these models and discuss how metamorphic basement is deformed under shallow condition. Hereafter, we present new structural analyses, cross-sections, and thin sections allowing to discuss the structural evolution of the Sierra Pie de Palo at various scales.

4. Structural analysis of the eastern Pie de Palo

One of the most peculiar features of the eastern side of the Pie de Palo range corresponds to several occurrences of range-facing, ~N-S striking escarpments (**Fig. 3c, 5, and 6**). These escarpments result from the Neogene to Quaternary activity of W-verging reverse faults that are parallel to the toe of the topography at several places. These faults are quite puzzling because their vergence apparently disagrees with the present topography as their relative vertical movement uplifts the South Bermejo Valley respect to the Sierra Pie de Palo. These faults have been interpreted as the discontinuous surface trace of a major E-dipping, reverse fault, which would ramp off from a deep décollement related to the western border fault of the Valle Fértil – La Huerta range (Ramos & Vujovich, 2000; Ramos, Cristallini & Pérez, 2002). To better understand the meaning of these faults, we have mainly focus our observations in two areas: Niquizanga (**Fig. 5**) and Ampacama (**Fig. 6**).

4.1. The Niquizanga area

In this area, two ~5-km long, basement ridges are observed (**Fig. 5, 7a**): the western Niquizanga and the eastern La Posta ridges. These two ridges are asymmetric with a western steep slope bordered on the West by reverse faults while their eastern slope corresponds to the Neogene unconformity. At both ridges, the basement overthrusts the Neogene sediments. These layers present a syncline geometry in the footwall, with a shallow East-dipping limb (e.g., 07°E close to site 17, **Fig. 5**) and a steep to vertical West-dipping one (e.g., 90° close to site 2, **Fig. 5**), attesting for W-verging kinematics for the fault. These faults are at least 6 km long and cannot be extended along more than 10 km. Based on their ~200-m high escarpment and the 10° E dip of the erosion surface below the Neogene sediments, the maximum fault displacement can be estimated to up to 500 m. This Niquizanga bounding fault reactivated an inherited pre-Andean shear zone (Niquizanga shear zone) that was active as an extensional structure during the Silurian (Mulcahy et al., 2011).

In the basement, small faults, located in the hangingwall of the main W-verging thrusts, are characterized by brittle deformation mainly parallel to the inherited metamorphic foliation. Microtectonic observations in the basement highlight a ENE-WSW contraction (sites 2, 6, 17, 23, 47, **Fig. 5**). This is consistent with the microtectonic observations in the sediments (ENE-WSW to ESE-WNW contraction, site 32, **Fig. 5**). Thus, it is most likely that the microfaults observed in the basement have the same age than the deformation seen in the late Tertiary-Quaternary sediments. Moreover, the shortening described above is also consistent with the overall N-S to NNE-SSW strike of the Pie de

Palo Anticline (**Fig. 5**), which is a late Tertiary-Quaternary feature. This also suggests that the brittle deformation observed in the basement is late Tertiary-Quaternary in age.

In addition, small-scale folds affecting both the sediments (site 32, **Fig. 5**) and the metamorphic foliation (site 2, 6, 23, **Fig. 5**) are oriented NNW-SSE to N-S. These data also strongly suggest that all the mentioned deformation (both in the basement and the Cenozoic strata) is Plio-Quaternary in age and consistent with an overall E-W shortening.

These folds and faults affecting the basement (**Fig. 8**) generally present W-verging kinematics consistent with the kinematics of the 2 main faults. Moreover, the folds are brittle in the sense that their hinges are very localized and consist of few fractures while the limbs are very planar (**Fig. 8b, c, 9a**). The folds also present kink geometries (**Fig. 8a**). These folds induce striations along the foliation planes (**Fig. 9b**), whose direction (roughly E-W) is also consistent with the E-W shortening. Finally, in the basement, one may also observe larger folds (metric-scale or more, **Fig. 9c**). These folds and their wavelength imply strong disharmony and several levels of decoupling inside the basement.

Parallel to the metamorphic foliation, breccias are also very frequent. They consist of brecciated elements from the basement attesting for shearing, with no or few cement (**Fig. 10a**). The same feature can be observed with higher amount of calcite cement (**Fig. 10b, c**). In thin section, one may clearly identify the original metamorphic rocks and newly formed calcite (**Fig. 11c, d**).

Brecciation, shearing, and small-scale folding seems strongly controlled by the anisotropy of the basement. Indeed, these structures are linked to levels of decoupling/decollement characterized by mica-rich layers (**Fig. 11a**) where brittle folds are rooting. Moreover, faults such as the La Posta Fault (**Fig. 5**) are clearly controlled by the inherited basement foliation: at its southern end, the fault turns systematically parallel to the inherited foliation. At larger scale, the La Posta fault also follows the inherited foliation: in the northern part, both the fault and the foliation are striking NNE-SSW; in the southern part, both the fault and the foliation are N-S.

On the eastern side of the section, the Neogene sediments (**Fig. 7a**) are gently dipping ~5-10°E. A 720 m-thick Neogene series has been described in the Niquizanga area (Cuerda, Varela & Iniguez, 1983), to the south of the La Posta Ridge (**fig. 5**). Accounting for the map width of these Neogene sediments and their average dip just to the north of the Niquizanga ridge, we calculated a rough estimate of some 600-700 m for the total Neogene thickness including the torrential conglomerates that are conformably topping the Neogene strata. This estimate is similar to the thickness calculated by Cuerda, Varela & Iniguez (1983), hence, they indicate that the Neogene and basement brittle deformation, which are observed in the Niquizanga area, were formed at less than 1 km depth. Finally, no tapering structures or progressive unconformity were observed within the Neogene series. Nevertheless, the Late Neogene, Rio del Camperito Formation (Cuerda, Varela & Iniguez, 1983), which is coarser than the underlying Niquizanga Formation (see above section 3), contains metamorphic clasts from the Sierra Pie de Palo basement. These clasts indicate that these coarser Late Neogene sediments are coeval with the onset of the basement uplift.

4.2. The Ampacama section

If this area is comparable to Niquizanga in the sense that it displays several W-verging reverse faults (**Fig. 6**), Neogene beds have steeper dips and the basement ridges are more numerous in the Ampacama area. Indeed, we mapped about 7 faults, 4 in the northern part affecting the basement and the Neogene deposits, 2 in the sedimentary cover affecting both Neogene beds and Quaternary alluvial strath terraces, and 1 in the southern part affecting the basement and the Neogene. These faults are NNW-SSE to N-S and dip at about 40°E (**Fig. 7b**) and even 76°E for the southernmost one. The faults observed in the sedimentary cover may affect the basement at depth. Although this cannot be observed, it is suggested because these faults stand in the southward prolongation of the easternmost basement ridge. Most of these faults are at least 3-4 km long and have displacement up to 500 m.

The faults in both the basement and the cover witness an E-W shortening (**Fig. 6**), which is consistent with the micro-faults reported for the southern Niquizanga area (**Fig. 5**).

In this area, it is noteworthy that several basement faults are parallel to the inherited metamorphic foliation, while some others are strongly oblique, or even perpendicular (**Fig. 7b**). Where the faults are oblique to the foliation, the later is not characterized by a strong mineralogical segregation, i.e., the foliation is particularly not underlined by mica-rich layers (**Fig. 11b**).

The sedimentary layers are folded in this area, mainly as synclines between the basement ridges. Along their western limb, the dips are about 20-40°E, while in the eastern limb, the dips can be up to 60-70°W. These geometries attest for significant asymmetries, that are also consistent with the W-verging basement thrusts.

Further west, in the Pie de Palo range, recent basement fault zones are also suspected (westernmost fault with a question mark, **Fig. 6, 7b**). These faults are characterized by intensively fractured and faulted rocks, with a clear W-verging kinematics. However, due to the lack of Neogene sediments, their age cannot be strictly constrained. It is noteworthy that, in this area in particular as well as few other ones, the basement foliation is not East-dipping, but is rather vertical to West-dipping. Further south, the foliation is also clearly folded: indeed, the orientation changes a lot in a rather restricted area (**Fig. 6**).

In the southernmost part of Ampacama, the sedimentary layers have dips increasing westward (from 20 to 65° and even vertical at few places, **Fig. 6**, southern part). In the area where the Neogene layers are steeper (50 to 62°E), a sub-vertical basement slice (89°E) crops out. On its western side, a very steep (62°E) W-verging fault can be observed at the contact with the Neogene (**Fig. 6**). In this area, where the Neogene beds show steeper dips than in the southern Niquizanga area, the basement reverse faults affecting the Neogene also tend to be steeper.

As in the Niquizanga area, the Neogene series is composed of two sedimentary formations that are conformably capped by Early Quaternary alluvial conglomerates (**Fig. 6**). No detailed study is available on this Neogene series. Using the same kind of method that in the Niquizanga, we calculated two rough estimates for the Neogene maximum thickness: a first one of ~900 m to the east of the eastern basement ridge and a second one of ~1100 m on the southern part of the Neogene outcrop. These two estimates suggest the thickness of the Ampacama Neogene series is on the order of 1000 m, hence slightly thicker than the Niquizanga Neogene formations. Nonetheless, the Ampacama thickness estimates also indicate that the Neogene deformation seen within the basement was formed under very shallow depth conditions. As in Niquizanga, the Neogene layers are characterized by lower dips on the eastern side of the section (between 20-35°E) while they show steeper (between 40-65°E) dips in the western part of the section (**Fig. 7a**). No progressive unconformities or sedimentary tapering were observed in the field. Nevertheless, as in Niquizanga, the Upper Neogene Rio del Camperito Formation is coarser and contains clasts of metamorphic rocks derived from the Sierra Pie de Palo. This indicates that the basement of the Pie de Palo range was actively uplifting and under erosion during the Upper Neogene.

4.3. Synthesis

To sum up, here are our main observations. At two locations, small (in both length and displacement) W-verging reverse faults are mapped East of the Sierra Pie de Palo: these faults have lengths ranging between 2 and 6-7 km but can hardly reach 10 km, their displacements are usually less than about 500 m. Compared to the length of the Pie de Palo Range, these faults are typically second order structures. Most of these faults reactivated the inherited metamorphic foliation and/or shear zones, especially along mica-rich levels with an oriented fabric (**Fig. 11a**). Along these planes, close to and above the reverse faults, we observed foliation-parallel slip, breccias and folded foliation planes in between. The kinematics of these structures is consistent with both the micro-faults measured within the sediments and the faults showing basement over sediments, as well as the overall geometry of the Pie de Palo range. This kinematics is also similar to that obtained from the inversion of earthquake focal mechanisms (Siame et al., 2005). It is noteworthy that this top-to-the-West kinematics is most likely not inherited from pre-Andean as Paleozoic top-to-the-East kinematics and associated lineations where observed in the Niquizanga shear zone. Thus, the reverse, top-to-the-West movement is most probably Neogene.

These W-verging faults have displacement ranging between a couple of hundreds meters and a maximum of 500 m. At some places (**Fig. 6**, southern part), the upward fault propagation is accompanied by gentle folds within the Neogene. Displacements in the Quaternary strath terraces are always much lower than within the Neogene formations. The northward prolongation of the Niquizanga basement ridge is at the limit of identification within the Quaternary alluvial surface. On the other hand, the surface of the Quaternary alluvial does not appear affected by the northward prolongation of the Posta Ridge, while the underlying Neogene is still tilted (**Fig. 5**). In the Ampacama area, where the Neogene beds are more deformed, a tier of Middle to Late Quaternary strath terraces is conspicuously gently folded, the highest, hence oldest surface terrace showing steeper dips in comparison to the younger ones. Nevertheless, the Quaternary terraces displacements and dips are significantly much smaller than those observed within the Neogene. All these data provide clear evidence that these W-vergent reverse faults are typically early within the deformation timing of the Sierra Pie de Palo. Moreover, the fact that steeper fault dips are always associated with the steeper Neogene dips also strongly suggests that these second order faults are early in the folding timing of the Sierra Pie de Palo

In between the two described area, neither basement rocks nor reverse faults are clearly identified along the central-eastern side of the Sierra Pie de Palo. The only dubious candidate for such a faulted basement ridge could stand in the Casas Viejas area (31.38°S; 67.81°W) (**Fig. 3b**). However, it is difficult to decipher in this area between the Neogene beds and a highly hydrothermal-altered basement. Either such basement ridges are present but buried below the Neogene beds or they did not develop similarly in the central part of the fold as in the areas of Niquizanga and Ampacama. It is worth to mention that similar range-facing scarps, striking NW-SE, are also observed within Quaternary alluvial fans of the NE corner of the Pie de Palo range (31.09°S; 67.8°W), 5-7 km to the SE of the Pajaritos fault (**Fig. 2, 3**).

All these observations suggest that E-W shortening was accommodated at the surface in several places by shear along foliation planes and inherited shear zones. In the next section, we detail how these newly created shear zones reactivating the foliation may evolve through time, how the Sierra Pie de Palo developed, and what implications it has for the crustal structure.

5. Mode of upper crustal shortening

5.1. Foliation-parallel shear

We showed above that most of the small reverse faults observed along the eastern side of the Sierra Pie de Palo initiated as foliation-parallel shear zone, controlled by (i) the inherited anisotropy of the foliation and (ii) the presence of low-strength mineral phases such as micas.

Micas are weak mineral phases and few experimental works have underlined that mica-rich aggregates are weaker than other rocks (such as quartzo-feldspathic ones) over a broad range of midcrustal depths (Shea & Kronenberg, 1992). Although the deformation at Sierra Pie de Palo occurred at much shallower depth than mid-crust, we may assume that the micas also behave as weak phases at shallow depths. In this case, they would allow accommodating large amount of strain, hence localizing the deformation and constituting shear zones.

Probably more significant than the intrinsic mechanical properties of these mineral phases, their anisotropy has been shown to control the rock strength. Indeed, in rock mechanics experiments, the weakening is controlled by the orientation of micas relative to the stress orientation (Shea & Kronenberg, 1993). This means that the softening is controlled by both the presence of micas (or any other phyllosilicate) and, more importantly, their arrangement (e.g., Bos & Spiers, 2001; Bos & Spiers, 2002; Niemeijer & Spiers, 2005; Jefferies et al., 2006; Collettini et al., 2009; Niemeijer, Marone & Elsworth, 2010; Holdsworth et al., 2011).

Hereafter, we propose a field-based conceptual model for the evolution of mica-rich foliated basement rocks deformed at low depths (**Fig. 12**). Initially, the foliation has overall a shallow dip (i.e., before Late Neogene folding), then, it is activated as reverse shear zones (**Fig. 12b**) on weak mica layers. At small-scale, these weak layers act as local decollement and thin quartzo-feldspathic layers start forming asymmetric folds consistent with the sense of shear (**Fig. 12b**). If deformation continues, the folded thin quartzo-feldspathic layers evolve as breccias subsequently more or less cemented by calcite (**Fig. 12c**). Ultimately, this zone can turn into a localized zone of shear. Thus, at larger scale, once this zone can accommodate significant deformation, it may act as a decollement level for larger folds involving a thicker pile of metamorphic rocks (**Fig. 9c, 12d**). This model accounts for the discrete shear zones/faults, large as well as small folds observed in the field.

This model assumes that the deformation seen in the hangingwall of the main reverse faults that can be interpreted as "immature" structures that formed the reverse faults. Thus, foliation-parallel slip was localized along the main reverse faults as well as distributed in their hangingwall (and footwall?). Additionally, some reverse faults are simply the reactivation of inherited shear zones (see above, Niquizanga thrust). The reactivation of other inherited Pampean thrusts/shear zones was already suggested from seismic line interpretation in the W-verging model (Verges et al., 2007).

As mentioned in section 4, these structures formed at very shallow depth, i.e., approximately 1 km, based on the estimated thickness of the Neogene sediments around Sierra Pie de Palo. This explains why only very brittle structures are observed, such as very localized shear zones, faults, brittle folds with very localized and fractured hinges, planar limbs, and breccias (**Fig. 8, 9, 10**).

At such shallow depth, the basement rocks are usually deformed in a very localized mode, i.e., with large faults or a series of smaller ones (e.g., Handy, Hirth & Hovius, 2007; Scholz, 2002). For the Pie de Palo Range, along with the small thrusts mapped in the field, the main feature is the anticline shape of this range, especially highlighted by relicts of the pre-Neogene erosional surface (Siame et al., 2015). In the next section, we discuss the mode and kinematics of such a basement shortening.

5.2. Fault vergence at the Sierra Pie de Palo

The deformation of the eastern Sierra Pie de Palo consists of several W-verging reverse faults. These faults, which have small lengths (2-8 km) and small displacements (less than 0.2 to 0.5 km), are shortly spaced (0.5-3 km) and correspond mostly to foliation-parallel, brittle shear zones that start developing within weak foliation levels of the basement during the early stage of folding. Consequently, their significance needs to be discussed in the framework of the folding models, which have been proposed for the Pie de Palo Anticline, i.e., W-verging fault bend fold (Ramos, Cristallini & Pérez, 2002; Vergés et al., 2007) or E-verging fault-propagation fold whose blind thrust branches at depth on a W-verging thrust (Siame, Bellier & Sebrier, 2006; Siame et al., 2002) or not (Kadinski-Cade and Reilinger, 1985), especially in terms of mechanism that distributes deformation in the basement.

According to Ramos, Cristallini & Pérez (2002) , the W-verging Niquizanga Fault (at Niquizanga Ridge, **Fig. 5, 7**), which is located at the rear of the Pie de Palo fault-bend fold, is a rather steep reverse fault ramping off below the eastern South Bermejo Basin, at more than 20 km depth. Such a fault contradicts the long-term topography (the southern Bermejo Valley should be uplifted and the Sierra Pie de Palo should be subsiding) and could only fit with an out-of-sequence structure. However, this option disagrees with our observations because the W-verging faults have short lengths, appear tilted with the sedimentary bedding, and can thus hardly ramp off at 20 km. Moreover, their displacement predates or more likely is coeval with the folding, hence partly early in the deformation timing of the Pie de Palo Anticline.

Another alternative associated with a fault bend fold might correspond to what was proposed for the Alpine basement units in the Pyrenees Axial Zone (Casas et al., 2003). There, steep Meso-Cenozoic faults affect both the basement and its Mezosoic cover. They are interpreted as faults initiated in the basement where it passed above a flat-ramp-flat system. Indeed, in such a case, the structural configuration and kinematics implies internal deformation within the basement (Casas et al., 2003). Such model could be contemplated for the Pie de Palo Anticline assuming a fault-bend fold (Ramos, Cristallini & Pérez, 2002; Vergés et al., 2007). Where the basement passes above a flat-ramp or a ramp-flat transition, there might be either contraction or extension in the upper unit, respectively. The W-verging reverse faults observed in the field might then witness this later configuration. However, this would imply that they formed at depth as the flat-ramp transition is in the deep crust. This is unlikely given the brittle structures observed in the field.

Considering that these small W-verging faults are observed in the eastern part of the Pie de Palo Anticline, which corresponds to a forelimb accounting for the shape of the erosional surface (**Fig. 3**), makes necessary to test the E-verging fault propagation fold model. In such a model, the W-verging faults could represent intercutaneous structures as it has been observed at several places (e.g., Mackay et al., 1996). If it is so, the slip on an E-verging blind basement fault would be distributed on several W-verging small basement faults. However, one expects such intercutaneous wedge structure should develop rather lately in the deformation timing. Thus, this option remains possible but not very likely because our observations suggest these small W-verging faults started to develop early in the sequence of shortening.

Considering that these small W-verging reverse faults are located in the forelimb of the Pie de Palo Anticline, where the dips are the steepest (30-90°), one can surmise that they are linked to a mechanism of folding. This fault pattern being due to foliation-parallel slip resembles the bedding-parallel slip in flexural-slip fold model. The role of basement preexisting fabric has been highlighted in several basement-cored folds (Schmidt, Genovese & Chase, 1993). The mode of folding described above may belong to the "mode 2" of Schmidt, Genovese & Chase (1993). However, in this later work, the fabric allowed the deformation to be distributed in the basement in the sense that the zone of deformation below the forelimb is large. Nonetheless, the mode of deformation is not folding *s.s*. It rather corresponds to a distributed mode of faulting that induced a fold in the overlying sedimentary cover.

Such a zone of deformation in the basement has been described at few places and often interpreted as a triangular shear zone, large toward the basement top, rooting and thinning downward in the upper tip of a thrust. Such model has been generalized for the sedimentary rocks by Erslev (1991) as a trishear mode of folding and applied for the basement to explain distributed faulting below the basement-cover interface (Bump, 2003; Garcia & Davis, 2004). If the fault upper tip is initially located into the basement, there might be, near the fault tip, a triangular zone of distributed deformation active until the fault potentially propagates to the basement/cover interface. In this zone, the basement may deform by pervasive faults and fractures, either pre-existing or newly created (Garcia & Davis, 2004); this induces a curved basement-cover interface because of distributed deformation. If such model applies for Sierra Pie de Palo, an E-verging basement thrust should terminate upward with a distributed zone of shear characterized by W-verging small faults.

Such switch of vergence makes the trishear model unlikely for the Sierra Pie de Palo, although it cannot be ruled out. Thus, finally, the small W-verging faults more probably witness a foliation parallel-slip mode of folding associated to an E-verging fault-propagation fold, similarly to what has been proposed for sedimentary rocks (Suppe & Medwedeff, 1990). Above the blind thrust tip, a fold developed to accommodate shortening. In this fold, the mode of folding, i.e., the way the distributed deformation is accommodated, is characterized by slip along inherited foliation planes (or inherited shear zones). Even if our observations cannot provide any kind of evidence to root a trishear model, one cannot totally discard it where the E-verging fault tip propagates at depth. In such a case it would coexist with the foliation-parallel slip model we propose for the Pie de Palo Anticline.

Interestingly, unfolding the Neogene Pie de Palo Anticline reveals a preexisting series of antiforms and synforms (**Fig. 13a**) suggesting that the Neogene and Quaternary shortening should have amplified inherited basement antiformal geometries (**Fig. 13b**): in the western part of the Sierra, the inherited foliation appears folded, with dips much higher than the erosional surface (**Fig. 3, 7, 13**). In the western Pie de Palo limb, several pre-Andean East-dipping thrusts are mapped and most of them are associated to East-dipping foliation (e.g., Van Staal et al., 2011; Mulcahy et al., 2011). However, West-dipping foliation can also be observed at some places (e.g., Van Staal et al., 2011; Mulcahy et al., 2011), especially at the Sierra top (Ramos & Vujovich, 2000). Thus, in the western limb, a series of antiforms and synforms of foliation is inherited, while at the Sierra top and in the eastern limb, a single asymmetric antiform is inherited from pre-Andean event (**Fig. 13**). Thus, we propose that the foliation-parallel slip mechanism for folding is relevant and could be the main folding mechanism giving the present-day shape of the Pie de Palo Anticline. In such a case, as mentioned above, this mechanism would somewhat resemble the flexural-slip model, hence, foliation-parallel slip in the basement would play the role of bedding-parallel slip in the cover. To accommodate the shortening in a flexural-slip fold, there is partitioning between bedding-parallel slip and layer internal deformation (fractures, veins, pressure-solution, twinning). In our model of foliation-parallel slip mode of folding, there is also a partitioning between slip along inherited foliation planes (reverse faults, **Fig. 7, 12, 13**) and internal deformation of basement rocks (here, fractures mainly, **Fig. 8 and 9**). Such deformation is most likely similar to that observed in the field: "brittle" folds with planar limbs and localized hinges (**Fig. 8 and 9**).

It is noteworthy that the reverse faults interpreted as witnessing flexural-slip mechanism are spaced of about few hundred meters to about a couple of km (**Fig. 5, 6**). This fits well with the fact that the displacements along these faults are on the order of about few hundred meters (**Fig. 7**), as predicted in Alonso et al. (1989).

At some places where the foliation was previously intensively folded, at smaller scale than the basement antiform (see spatial variations of foliation orientation in Fig. 5.), new faults were laterally propagated and created oblique to the local foliation, to ensure a kinematics consistent at fold scale.

Therefore, the W-verging small reverse faults seen along the eastern side of the Pie de Palo anticline agree with an E-verging fault propagation fold. Moreover, the dip of the Neogene series in the eastern Pie de Palo is very high at some places (more than 60°, **Fig. 6**), which does not fit well with a fault-bend fold model where such dips should represent the dip of the W-verging thrust. Thus, although the W-verging model, cannot be totally discarded we have shown that structural data permit to suggest an alternative model with a major crustal blind thrust and an associated fault-propagation fold (**Fig. 13, 14**). Moreover, this surmised major crustal blind thrust is quite consistent with local microseismic data (Regnier et al., 1992) showing a W-dipping alignment of foci (average dip around 30-35°E), especially in the northern part of Pie de Palo (**Fig. 4a, 13, 14**). Two mechanisms can fit with this latter structural model: intercutaneous faults or foliation-parallel slip mechanism, this second mechanism being much more likely. Finally, the Neogene Pie de Palo fold appears to have developed on inherited basement antiformal and synformal geometries.

6. Crustal and lithospheric structure

Our mains results are twofold: first, we show how the inherited metamorphic foliation controlled and influenced the formation of small faults in the basement, and second, we argue that the overall kinematics of the Sierra Pie de Palo as well as the depth distribution of seismic foci are consistent with an E-verging fault-propagation crustal fold. In the following sections, we propose a more speculative discussion at both crustal and lithospheric scales.

6.1. Crustal implications

We have proposed that the dominant folding mechanism should be foliation-parallel slip and that it induced the formation of small reverse faults, the foliation being not parallel to the basement-cover interface. Such interpretation has also been proposed for other Andean structures (e.g., Alonso et al., 2005). Alternatively, these small structures may also be due to intercutaneous wedge processes. However, in both cases the resulting crustal thrust should be E-verging. It is noteworthy that an E-verging blind thrust below the Sierra Pie de Palo is opposite to the main kinematics of the Pampean province.

According to seismological data, we consider here that the E-verging blind thrust below the Sierra Pie de Palo should root at the base or below the upper seismogenic crust, i.e., at ~40 km (**Fig. 14c**) as already proposed by Siame et al. (2015) for a slightly different structural interpretation (**Fig. 14b**). In our model, the thrust to the SW of the Sierra Pie de Palo (Tulum Fault) is considered as a back thrust branched at depth on the main E-verging thrust. This configuration is in agreement with the seismicity (**Fig. 13, 14**), especially considering that the 1977 earthquake should be located 30 km west (**Fig. 14c**) of its initial location (**Fig. 14a, b**) as stated in Regnier et al. (1992). The 20°E dip of the erosional surface (backlimb west of the Tulum W-verging thrust, below the Neogene sediments of the Tulum valley, **Fig. 2, 13a, 14**) thus approximately represents the dip of the E-verging thrust at depth, consistently with the model of fault-propagation fold.

The E-verging thrust ramp off a deep crustal decollement (either at the base of the seismogenic crust or in the lower crust, **Fig. 14c**) as well as the E-verging basement thrust that activated the Eastern Precordillera (Meigs et al., 2006). This Precordillera is W-verging because of the change of vergence in the decollement at the base of the cover (**Fig. 14c**). This is consistent with the interpretation of Vergés et al. (2007), Meigs et al. (2006), and Rockwell et al. (2014), if we consider that the 1944 earthquake is due to a displacement at the cover base where the thrust vergence changes (**Fig. 14c**) at 9 to 11 km (Alvarado & Beck, 2006; Meigs et al., 2006). Alternatively, this 1944 earthquake could have ruptured deeper (~25 km) on the E-verging basement ramp (Meigs & Nabelek, 2010), which is located below the Eastern Precordillera (Smalley et al., 1993) (**Fig. 14c**).

These two E-verging structures, which are located below the Eastern Precordillera and the Pie de Palo Anticline, stand between the thin-skinned Western and Central Precordillera to the West and the Pampean W-verging Sierra de Valle Fértil to the East.

It is noteworthy that the crust below the Sierra Pie de Palo and the Valle Fértil is considered as different (e.g., Ramos, 2004): the crust below Valle Fértil and further East is Pampia, while below Sierra Pie de Palo and the Precordillera it is Cuyania. Thus, there might be a link between these different crusts and the different vergences in these domains: in the Cuyania domain, the thrusts are E-verging at the surface (except in the Eastern Precordillera) while in the Pampia crust, the thrusts appear predominantly W-verging.

6.2. Lithospheric structure

In the North-American Laramide province of the Rocky Mountains, the presence of large basement uplift (similar to the Sierras Pampeanas, e.g., Jordan & Allmendinger, 1986) is probably due to subcrustal shear, crustal buckling and faulting above a decollement in the lower crust, or crustal buckling and faulting superimposed to a lithosphere buckling (Erslev, 2005; Yonkee & Weil, 2015; see a synthesis in Lacombe & Bellahsen, this issue). In all cases, the driving force arises from the push of a flat slab transmitting stresses far in the interior of the overriding plate. In the Andean foreland of North-western Argentina, both vergences are found in the mountain range and are most likely controlled by inherited structures (Ramos, Cristallini & Pérez, 2002).

The E-verging thrusts beneath the Sierra Pie de Palo and the Eastern Precordillera could be considered as a “normal kinematics”: they are the eastward thick-skinned propagation at depth of the E-verging thin-skinned system of the Precordillera. As classically considered, the flat slab geometry induced stresses to be propagated farther down in the crust and to the East. The W-verging Pampean structures (such as Valle Fértil) are strongly controlled by structural inheritance, i.e., E-dipping inherited Triassic normal faults that are reactivated during the Neogene and Quaternary (Ramos, Cristallini & Pérez, 2002).

The Cuyania crust below the Sierra Pie de Palo is very thick (52-60 km), while the thickness of the Pampean crust, farther east, decreases eastward from ~50 km to 35 km (Ammirati, Alvarado & Beck, 2015; Ammirati et al., 2013). Moreover, these authors interpreted the Cuyania lower crust as eclogitized. As the shortening is rather low in this region (**Fig. 13**), it cannot only explain the eclogitization; it should rather result from the initial thickness of the Cuyania crust. Thus, it is likely that Cuyania was already quite thick at least in its eastern part, before the Neogene shortening.

Below the Precordillera, the crust is thicker (~65 km, e.g., Ammirati et al., 2013). Considering the amount of shortening in the Precordillera (135 km), the Cuyania crust must have been significantly underthrusted below the Andean Cordillera, i.e., below the Chilenia upper crust (Cristallini & Ramos, 2000). Thus, it is likely that, for balancing purpose, the Chilenia lower crust was underthrusted below Cuyania (Cristallini & Ramos, 2000) (**Fig. 15**). This process is coeval with the Tertiary formation of the Principal and Frontal Cordilleras as well as the Western and Central Precordilleras. During this process, the Chilenia lower crust was possibly eclogitized as well as the Cuyania lower crust farther east.

When the slab dip decreased, at about 10 Ma, the stresses were transferred to the Cuyania and Pampia crust. It is noteworthy that it may also correspond to the period when the crust below the Cordillera and Precordillera became too thick and too strong because of its eclogitized root. The shortening propagated through a deep decollement between the seismogenic crust and the eclogitized root, in the Cuyania crust at ~40 Km depth, and farthermost to the Sierra de Córdoba region within the Pampia/Rio de la Plata crusts at about 35 km depth.

7. Conclusions

We have investigated the small W-verging reverse faults along the eastern side of the Sierra Pie de Palo Anticline. We show that these faults are less than 8 km-long and have displacement of few hundreds of meters. These faults are thus relatively shallow and can hardly root in the deep crust as previously proposed (e.g., Ramos, Cristallini & Pérez, 2002). These faults show typical brittle structures in the basement. They initiated in the basement by shearing along inherited weak foliation levels or inherited shear zones, particularly within mica-rich layers, inducing a small scale folding of quartz-feldspathic layers, and subsequently their brecciation. They evolved as thrust faults propagating in the Neogene cover as thrusts or folds, and are even faulting Quaternary strath terraces.

These faults, which are only seen along the eastern side if the Sierra Pie de Palo, may attest for basement folding at crustal-scale, with foliation-parallel slip as folding mechanism, although alternative models may also be considered. The highly deformed eastern Sierra Pie de Palo most likely represents a forelimb and thus suggests for E-verging blind thrust at depth. This vergence is opposite to the common Pampean vergence but may be considered as typical for Cuyania crust.

Such E-verging thrust may be rooting at depth westward beneath the Andean Cordillera (as well as the other Pampean W-verging thrusts, linked through a mid- to lower-crustal décollement) where the Chilenia lower crust is underthrusted and eclogitized below the Cuyania crust.

Acknowledgements

This work was made within a joint program between ISTeP (Sorbonne University-University Pierre and Marie Curie, Paris) and CEREGE (Aix en Provence). SPOT images were provided by Tectoscope-Andes and ISIS programs (CNES/INSU/CNRS). We thank ECOS-SUD program for travel grants allowed to N. Bellahsen, M. Sébrier, and L. Siame for field work in Argentine. We are in debt to Carlos Costa (Universidad Nacional de San Luis), for logistical help and many discussions on the geology of the Sierra Pampeanas and Argentina in general. We also thank E. Ahumada and H. Cisneros for very valuable help during fieldwork and J. L. Alonso and an anonymous reviewer for their comments that greatly improved the initial version of the manuscript.

References

ALONSO, J. L. 1989. Fold reactivation involving angular unconformable sequences: Theoretical analysis and natural examples from the Cantabrian zone (northwest Spain). *Tectonophysics* **170**, 57-77.

ALONSO, J.L., RODRIGUEZ_FERNANDEZ, L.R., GARCIA-SANSEGUNDO, J., HEREDIA, N., FARIAS, P. and GALLASTEGUI, J. (2005).- Gondwanic and Andean structure in the Argentine Central Precordillera: the Río San Juan section revisited. 6th International Symposium on Andean Geodynamics. IRD Editions (Institut de Recherche pour le Développement), Extended Abstracts, Paris, 36–39

ALLMENDINGER, R.W., FIGUEROA, D., SNYDER, D., BEER, J., MPODOZIS, C. & ISACKS, B.L. 1990. Foreland shortening and crustal balancing in the Andes at 30°S Latitude. *Tectonics* **9**, 789–809.

ALVARADO, P. & BECK, S. 2006. Source characterization of the San Juan (Argentina) crustal earthquakes of 15 January 1944 (Mw 7.0) and 11 June 1952 (Mw 6.8). *Earth and Planetary Science Letters* **243**(3-4), 615–631.

ALVARADO, P., BECK, S., ZANDT, G., ARAUJO, M. & TRIEP, E. 2005. Crustal deformation in the south-central Andes backarc terranes as viewed from regional broad-band seismic waveform modelling. *Geophysical Journal International* **163**(2), 580–598.

ALVARADO, P., BECK, S. & ZANDT, G. 2007. Crustal structure of the south-central Andes Cordillera and backarc region from regional waveform modelling. *Geophysical Journal International* **170**(2), 858–875.

ALVARADO, P., PARDO, M., GILBERT, H., MIRANDA, S., ANDERSON, M., SAEZ, M. & BECK, S. 2009. Flat-slab subduction and crustal models for the seismically active Sierras Pampeanas region of Argentina. In *Geological Society of America Memoirs*, pp. 261–278.

AMMIRATI, J.-B., ALVARADO, P., PERARNAU, M., SAEZ, M. & MONSALVO, G. 2013. Crustal structure of the Central Precordillera of San Juan, Argentina (31°S) using teleseismic receiver functions. *Journal of South American Earth Sciences* **46**, 100–109.

AMMIRATI, J.-B., ALVARADO, P. & BECK, S. 2015. A lithospheric velocity model for the flat slab region of Argentina from joint inversion of Rayleigh wave phase velocity dispersion and teleseismic receiver functions. *Geophysical Journal International* **202**(1), 224–241.

ANDERSON, M., ALVARADO, P., ZANDT, G. & BECK, S. 2007. Geometry and brittle deformation of the subducting Nazca Plate, Central Chile and Argentina. *Geophysical Journal International* **171**(1), 419–434.

BEAUDOIN, N., LEPRETRE, R., BELLAHSEN, N., LACOMBE, O., AMROUCH, K., CALLOT, J.-P., EMMANUEL, L. & DANIEL, J.-M. 2012. Structural and microstructural evolution of the Rattlesnake Mountain Anticline (Wyoming, USA): New insights into the Sevier and Laramide orogenic stress build-up in the Bighorn Basin. *Tectonophysics* **576-577**, 20–45.

BOS, B. & SPIERS, C.J. 2001. Experimental investigation into the microstructural and mechanical evolution of phyllosilicate-bearing fault rock under conditions favouring pressure solution. *Journal of Structural Geology* **23**(8), 1187–1202.

BOS, B. & SPIERS, C.J. 2002. Frictional-viscous flow of phyllosilicate-bearing fault rock: Microphysical model and implications for crustal strength profiles. *Journal of Geophysical Research* **107**(B2).

BROOKS, B.A., BEVIS, M., SMALLEY, R., KENDRICK, E., MANCEDA, R., LAURIA, E., MATURANA, R. & ARAUJO, M. 2003. Crustal motion in the Southern Andes (26°-36°S): Do the Andes behave like a microplate? *Geochemistry, Geophysics, Geosystems* **4**(10), n/a–n/a.

BUMP, A.P. 2003. Reactivation, trishear modeling, and folded basement in Laramide uplifts: Implications for the origins of intracontinental faults. *GSA Today* **March**, 4–10.

CAHILL, T. & ISACKS, B.L. 1992. Seismicity and Shape of the Subducted Nazca Plate. *Journal of Geophysical Research* **97**, 17,503–17529.

CALKINS, J.A., ZANDT, G., GILBERT, H.J. & BECK, S.L. 2006. Crustal images from San Juan, Argentina, obtained using high frequency local event receiver functions. *Geophysical Research Letters* **33**(7).

CARIGNANO, C., CIOCCALE, M. & RABASSA, J. 1999. Landscape antiquity of the Central-Eastern Sierras Pampeanas (Argentina): Geomorphological evolution since Gondwanic times. *Z. Fur Geomorphologie Suppl.* **118**, 245–268.

CASAS, A., OLIVA, B., ROMAN-BERDIEL, T. & PUEYO, E. 2003. Basement deformation: tertiary folding and fracturing of the Variscan Bielsa granite (Axial zone, central Pyrenees). *Geodinamica Acta* **16**(2-6), 99–117.

COLLETTINI, C., NIEMEIJER, A., VITI, C. & MARONE, C. 2009. Fault zone fabric and fault weakness. *Nature* **462**(7275), 907–910.

COLLO, G., DAVILA, F.M., TEIXEIRA, W., NOBILE, J.C., SAN'T ANNA, L. & CARTER, A. 2015. Isotopic and thermochronologic evidence of extremely cold lithosphere associated with a slab flattening in the Central Andes of Argentina. *Basin Research*, n/a–n/a.

COSTA, C.H., GARDINI, C.E., DIEDERIX, H. & CORTES, J.M. 2000. The Andean orogenic front at Sierra de Las Peñas-Las Higueras, Mendoza, Argentina. *Journal of South American Earth Sciences* **13**(3), 287–292.

CRISTALLINI, E.O. & RAMOS, V.A. 2000. Thick-skinned and thin-skinned thrusting in the La Ramada fold and thrust belt: Crustal evolution of the High Andes of San Juan, Argentina (32 SL). *Tectonophysics* **317**(3), 205–235.

CUERDA, A., VARELA, R. & INIGUEZ, A.M. 1983. Secuencia salifera en el terciario de Nikisanga, Sierra Pie de Palo, Provincia de San Juan. *Asociacion Geologica Argentina* **38**, 412–420.

DAVILA, F.M. & CARTER, A. 2013. Exhumation history of the Andean broken foreland revisited. *Geology* **41**(4), 443–446.

DEMETS, C., GORDON, R.G., ARGUS, D.F. & STEIN, S. 1990. Current plate motions. *Geophysical journal international* **101**(2), 425–478.

ENKELMANN, E., RIDGWAY, K.D., CARIGNANO, C. & LINNEMANN, U. 2014. A thermochronometric view into an ancient landscape: Tectonic setting, development, and inversion of the Paleozoic eastern Paganzo basin, Argentina. *Lithosphere* **6**(2), 93–107.

ERSLEV, E.A. 1991. Trichear fault-propagation folding. *Geology* **19**, 617–620.

ERSLEV, E.A. 2005. 2D Laramide geometries and kinematics of the Rocky Mountains, western USA. In *The Rocky Mountain Region: An Evolving Lithosphere. Tectonics,* *Geochemistry, and Geophysics*, pp. 7–20. Geophysical Monograph Series 154, Washington: K.E. Kalstrom & G.R. Keller.

GARCIA, P.E. & DAVIS, G.H. 2004. Evidence and mechanisms for folding of granite, Sierra de Hualfn basement-cored uplift, northwest Argentina. *AAPG bulletin* **88**(9), 1255–1276.

GUTSCHER, M.-A., MAURY, R., EISSEN, J.-P. & BOURDON, E. 2000. Can slab melting be caused by flat subduction? *Geology* **28**, 353–538.

HANDY, M., HIRTH, G. & HOVIUS, N. 2007. Continental fault structure and rheology from the frictional-to-viscous transition downward.

HOLDSWORTH, R.E., VAN DIGGELEN, E.W.E., SPIERS, C.J., DE BRESSER, J.H.P., WALKER, R.J. & BOWEN, L. 2011. Fault rocks from the SAFOD core samples: Implications for weakening at shallow depths along the San Andreas Fault, California. *Journal of Structural Geology* **33**(2), 132–144.

JEFFERIES, S.P., HOLDSWORTH, R.E., WIBBERLEY, C.A.J., SHIMAMOTO, T., SPIERS, C.J., NIEMEIJER, A.R. & LLOYD, G.E. 2006. The nature and importance of phyllonite development in crustal-scale fault cores: an example from the Median Tectonic Line, Japan. *Journal of Structural Geology* **28**(2), 220–235.

JORDAN, T.E. & ALLMENDINGER, R.W. 1986. The Sierras Pampeanas of Argentina: A modern analogue of Rocky Mountain foreland deformation. *American Journal of Science* **286**, 737–764.

JORDAN, T.E., ISACKS, B.L., RAMOS, V.A. & ALLMENDINGER, R.W. 1983. Mountain Building in the Central Andes. *Episodes* **3**, 20–26.

JORDAN, T.E., ZEITLER, P., RAMOS, V. & GLEADOW, A.J.W. 1989. Thermochronometric data on the development of the basement peneplain in the Sierras Pampeanas, Argentina. *Journal of South American Earth Sciences* **2**(3), 207–222.

JORDAN, T.E., ALLMENDINGER, R.W., DAMANTI, J.F. & DRAKE, R.E. 1993. Chronology of Motion in a Complete Thrust Belt: The Precordillera, 30-31°S, Andes Mountains. *The Journal of Geology* **101**, 135–156.

JORDAN, T.E., SCHLUNEGGER, F. & CARDOZO, N. 2001. Unsteady and spatially variable evolution of the Neogene Andean Bermejo foreland basin, Argentina. *Journal of South American Earth Sciences* **14**(7), 775–798.

KADINSKY-CADE, K. & REILINGER, R. 1985. Surface Deformation Associated With the November 23, 1977, Caucete, Argentina, Earthquake Sequence. *Journal of Geophysical Research* **90**, 12,691–12,700.

KAY, S.M. & ABBRUZZI, J.M. 1996. Magmatic evidence for Neogene lithospheric evolution of the central Andean 'flat-slab' between 30°S and 32°S. *Tectonophysics* **259**, 15–28.

KAY, S.M. & MPODOZIS, C. 2002. Magmatism as a probe to the Neogene shallowing of the Nazca plate beneath the modern Chilean flat-slab. *Journal of South American Earth Sciences* **15**, 39–57.

LACOMBE, O. & BELLAHSEN, N. 2016. Thick-skinned tectonics and basement-involved fold-thrust belts. Insights from selected Cenozoic orogens. *Geological Magazine,* doi:10.1017/S0016756816000078 (this issue)

LANGER, C.J. & BOLLINGER 1988. Aftershocks of the western Argentina (Caucete) earthquake of 23 November 1977: some tectonic implications. *Tectonophysics* **148**, 131–146.

LÖBENS, S., BENSE, F.A., WEMMER, K., DUNKL, I., COSTA, C.H., LAYER, P. & SIEGESMUND, S. 2011. Exhumation and uplift of the Sierras Pampeanas: preliminary implications from K–Ar fault gouge dating and low-T thermochronology in the Sierra de Comechingones (Argentina). *International Journal of Earth Sciences* **100**(2-3), 671–694.

LÖBENS, S., BENSE, F.A., DUNKL, I., WEMMER, K., KLEY, J. & SIEGESMUND, S. 2013.

Thermochronological constraints of the exhumation and uplift of the Sierra de Pie de Palo, NW Argentina. *Journal of South American Earth Sciences* **48**, 209–219.
MACKAY, P.A., VARSEK, J.L., KUBLI, T.E., DECHESNE, R.G., NEWSON, A.C. & REID, J.P. 1996. Triangle zones and tectonic wedges: An introduction. *Bulletin of Canadian Petroleum Geology* **44**, 1–5.
MEIGS, A., KRUGH, W.C., SCHIFFMAN, C., VERGES, J., RAMOS, V.A. & OTHERS 2006. Refolding of thin-skinned thrust sheets by active basement-involved thrust faults in the eastern Precordillera of western Argentina. *Revista de la Asociación Geológica Argentina* **61**(4), 589–603.
MEIGS, A.J. & NABELEK, J. 2010. Crustal-scale pure shear foreland deformation of western Argentina. *Geophysical Research Letters* **37**(11).
NIEMEIJER, A., MARONE, C. & ELSWORTH, D. 2010. Fabric induced weakness of tectonic faults. *Geophysical Research Letters* **37**(3), n/a–n/a.
NIEMEIJER, A.R. & SPIERS, C.J. 2005. Influence of phyllosilicates on fault strength in the brittle-ductile transition: insights from rock analogue experiments. *Geological Society of London Special Publications* **245**, 303.
MULCAHY, S. R., S. M. ROESKE, W. C. McCLELLAND, F. JOURDAN, A. IRIONDO, P. R. RENNE, J. D. VERVOORT, & G. I. VUJOVICH. 2011. Structural evolution of a composite middle to lower crustal section: The Sierra de Pie de Palo, northwest Argentina, *Tectonics* **30**, doi:10.1029/2009TC002656.
PERARNAU, M., GILBERT, H., ALVARADO, P., MARTINO, R. & ANDERSON, M. 2012. Crustal structure of the Eastern Sierras Pampeanas of Argentina using high frequency local receiver functions. *Tectonophysics* **580**, 208–217.
PILGER, R.H. 1981. Plate reconstructions, aseismic ridges, and low-angle subduction beneath the Andes. *Geological Society of America Bulletin* **92**, 448–456.
RABASSA, J.C., CARIGNANO, C. & CIOCCALE, M. 2010. Gondwana paleosurfaces in Argentina: An introduction, Geociencias. *Geociencas* **4**, 439–466.
RAMOS, V.A. 2004. Cuyania, an Exotic Block to Gondwana: Review of a Historical Success and the Present Problems. *Gondwana Research* **7**, 1–18.
RAMOS, V.A. & VUJOVICH, G. 2000. *Hoja Geológica San Juan, escala 1:250.000*
RAMOS, V.A., CRISTALLINI, E.O. & PEREZ, D.J. 2002. The Pampean flat-slab of the Central Andes. *Journal of South American Earth Sciences* **15**(1), 59–78.
REGNIER, M., CHATELAIN, J.L., SMALLEY, R., CHIU, J.-M., ISACKS, B.L. & ARAUJO, M. 1992. Seismotectonics of Sierra Pie de Palo, a basement block uplift in the Andean foreland of Argentina. *Bulletin of the Seismological Society of America* **82**(6), 2549–2571.
REILINGER, R. & KADINSKY-CADE, K. 1985. Earthquake Deformation Cycle in the Andean Back Arc, Western Argentina. *Journal of Geophysical Research* **90**, 12,701–12,712.
ROCKWELL, T.K., RAGONA, D.E., MEIGS, A.J., OWEN, L.A., COSTA, C.H. & AHUMADA, E.A. 2014. Inferring a Thrust-Related Earthquake History from Secondary Faulting: A Long Rupture Record of La Laja Fault, San Juan, Argentina. *Bulletin of the Seismological Society of America* **104**(1), 269–284.
SCHMIDT, C.J., GENOVESE, P.W. & CHASE, R.B. 1993. Role of basement fabric and cover-rock lithology on the geometry and kinematics of twelve folds in the Rocky Mountain foreland. In *Laramide basement deformation in the Rocky Mountain foreland of the western United States*, pp. 1–44. Geological Society of America Special Paper 280, C.J. Schmidt, R.B. Chase & E.A. Erslev.
SCHOLZ, C.H. 2002. *The mechanics of earthquakes and faulting* Cambridge university press.,p.
SEBRIER, M., MERCIER, J.-L., MACHARE, J., BONNOT, D., CABRERA, J. & BLANC, J.-L. 1988. The state

of stress in an overriding plate sitiuated above a flat slab: The Andes of Central Peru. *Tectonics* **7**, 895–928.

SHEA, W.T. & KRONENBERG, A.K. 1992. Rheology and deformation mechanisms of an isotropic mica schist. *Journal of Geophysical Research: Solid Earth (1978–2012)* **97**(B11), 15201–15237.

SHEA, W.T. & KRONENBERG, A.K. 1993. Strength and anisotropy of foliated rocks with varied mica contents. *Journal of Structural Geology* **15**, 1097–1121.

SIAME, L.L., BELLIER, O., SEBRIER, M., BOURLES, D., LETURMY, P., PEREZ, M. & ARAUJO, M. 2002. Seismic hazard reappraisal from combined structural geology, geomorphology and cosmic ray exposure dating analyses: the Eastern Precordillera thrust system (NW Argentina). *Geophysical Journal International* **150**, 241–260.

SIAME, L.L., BELLIER, O., SEBRIER, M. & ARAUJO, M. 2005. Deformation partitioning in flat subduction setting: Case of the Andean foreland of western Argentina (28°S-33°S). *Tectonics* **24**(5).

SIAME, L.L., BELLIER, O. & SEBRIER, M. 2006. Active tectonics in the Argentine Precordillera and western Sierras Pampeanas. *Revista de la Asociación Geológica Argentina* **61**(4), 604–619.

SIAME, L.L., SEBRIER, M., BELLIER, O., BOURLES, D., COSTA, C., AHUMADA, E.A., GARDINI, C.E. & CISNEROS, H. 2015. Active basement uplift of Sierra Pie de Palo (Northwestern Argentina): Rates and inception from ^{10} Be cosmogenic nuclide concentrations. *Tectonics* **34**(6), 1129–1153.

SMALLEY, R.J., PUJOL, J., REGNIER, M., CHIU, J.-M., CHATELAIN, J.L., ISACKS, B.L., ARAUJO, M. & PUEBLA, N. 1993. Basement seismicity beneath the Andean Precordiellera thin-skinned thrust belt and implications for crustal and lithopsheric behavior. *Tectonics* **12**, 63–76.

SUPPE, J. & MEDWEDEFF, D.A. 1990. Geometry and kinematics of fault-propagation folding. *Eclogae Geologicae Helvetiae* **83**(3), 409–454.

VAN VAN STAAL, C. R., VUJOVICH, G. I., CURRIE, K. L., et al. 2011. An Alpine-style Ordovician collision complex in the Sierra de Pie de Palo, Argentina: Record of subduction of Cuyania beneath the Famatina arc. *Journal of Structural Geology* **33** (3), 343-361.

VERGES, J., RAMOS, V.A., MEIGS, A., CRISTALLINI, E., BETTINI, F.H. & CORTES, J.M. 2007. Crustal wedging triggering recent deformation in the Andean thrust front between 31°S and 33°S: Sierras Pampeanas-Precordillera interaction. *Journal of Geophysical Research* **112**(B3).

YANEZ, G.A., RANERO, C.R., VON HUENE, R. & DIAZ, J. 2001. Magnetic anomaly interpretation across the southern central Andes (32°-34°S): The role of the Juan Fernandez Ridge in the late Tertiary evolution of the margin. *Journal of Geophysical Research* **106**, 6325–6345.

YONKEE, W.A. & WEIL, A.B. 2015. Tectonic evolution of the Sevier and Laramide belts within the North American Cordillera orogenic system. *Earth-Science Reviews* **150**, 531–593.

ZAMBRANO, J.. & SUVIRES, G.M. 2008. Actualización en el lımite entre sierras Pampeanas occidentales y Precordillera Oriental, en la provincia de San Juan. *Rev. de la Asociac. Geol. Argentina* **63**, 110–116.

ZAPATA, T.R. 1998. Crustal structure of the Andean thrust front at 30°S latitude from shallow and deep seismic reflection profiles, Argentina. *Journal of South American Earth Sciences* **11**, 131–151.

ZAPATA, T.R. & ALLMENDINGER, R.W. 1996. Growth stratal records of instantaneous and progressive limb rotation in the Precordillera thrust blet and Bermejo basin, Argentina. *Tectonics* **15**, 1065–1083.

Figure caption

Figure 1: a) Map of Central Andes (Landsat images and General Bathymetric Charts of the Oceans) together with distribution of active volcanoes (orange solid triangles, Smithsonian Institution, Global Volcanism Program) and seismicity (red solid dots, U.S. Geological Survey seismicity catalog, M >= 4.0 and depth <=70 km). White solid lines (labelled in km) are isodepth of the Wadati-Benioff plane and highlight the Pampean Flat Slab of the Nazca Plate (after Ammirati et al., 2013). Keys: AP, Argentine Precordillera; SP, Sierras Pampeanas; JRF, Juan Fernandez Ridge. b) Schematic regional structural map of the Sierra Pampeanas. Red solid lines denote active structures. Keys: AP, Argentine Precordillera; WP, Western Argentine Précordillera; CP, Central Argentine Precordillera; EP, Eastern Central Precordillera; SPDP, Sierra Pie de Palo; SH, Sierra de la Huerta; SVF, Sierra de Valle Fèrtil; SMa: Sierra La Maz; SFa, Sierra de Famatina; SFi, Sierra Fiambalà; SA, Sierra Ambato; SV, Sierra Velasco; SCh, Sierra Chepes; SC, Sierra de Cordoba; SL, Sierra San Luis; SU, Sierra Umango; SPa, Sierra de las Planchadas.

Figure 2: Tentative schematic structural map of the Sierra Pie de Palo and surroundings showing the major faults. Modified after Siame et al. (2015). CF, Las Chacras Fault; EPF, East Pie de Palo Fault; LPF, Los Pajaritos Fault; NPF, North Pie de Palo Fault; SHF, Sierra de la Huerta Fault; TVF, Tullum Valley Fault; VFF, Valle Fertil Fault; VPF, Villicùm-Pedernal Fault. The dashed line East of the Pie de Palo is the limit between alluvial fans and the flat playa type of Quaternary sediments. Its linear geometry suggests that the

alluvial fans are slightly tilted; this should be controlled by the blind E-verging thrust. Indeed, the older fans surfaces are steeper than the younger ones (the older the fan, the steeper its surface). Light blue stars locate 1944 (Mw = 7.0) and 1952 (Mw = 6.8) earthquakes with focal mechanism solutions after Alvarado and Beck (2006). Black stars locate fore- and main shocks of the Caucete 1977 (Ms = 7.4) earthquake (focal mechanism solutions after Langer and Hartzell, 1996).

Figure 3: a) Landsat image of the Sierra Pie de Palo. Both ≈E-W (B-B′) and ≈N-S (C-C′) topographic cross-sections have been extracted from the SRTM90 DEM (thick solid lines). The reconstructed regional erosion surface (thick dotted lines) is after Siame et al. (2015). The two stars locate the two 1977 earthquakes with their respective focal solutions (F for fore shock and M for main shock) (Langer and Hartzell, 1996). Keys: GEM, Grande El Molle lineament; GL, Guayaupa-Lima lineament. b) Geological map with main foliation orientations modified from Ramos and Vujovich (2000), Mulcahy et al. (2011), and Van Staal et al. (2011).

Figure 4: Seismicity profiles below the Sierra Pie de Palo showing seismic foci in vertical cross-sections redrawn after Regnier et al. (1992). a) for the northern half of the sierra. b) for the southern half of the sierra. See in Regnier et al. (1992) for the original data and precise location of the earthquakes that were projected on the sections. See Fig. 3 for location of the cross-sections.

Figure 5: Structural data at Niquizanga. See Fig. 3 for location. This area mainly consists of two basement ridges due to W-verging thrust faults affecting both the basement and the Cenozoic sedimentary cover. The faults are NNE-SSW and attest for a ENE-WSW

shortening according to the microtectonic data. The kinematic data show axes of deformation in the basement consistent with those in the cover. Fold axes (black dots in the stereonets) are also consistent with an ENE-WSW shortening, both in the basement and the cover. In the investigated sites (white circles with numbers), the basement foliation dips eastward.

Figure 6: Structural data at Ampacama. See Fig. 3 for location. This area consists of two main basement ridges due to W-verging thrusts faults in the basement, thrusting above the Cenozoic sediments. The faults are NNW-SSE and attest for a E-W shortening according to the microtectonic data. The kinematic data show axes of deformation in the basement consistent with those in the cover. In the investigated sites (white circles with numbers), the basement foliation usually dips eastward, although at several places it is either vertical or west-dipping.

Figure 7: Cross-sections through both investigated areas. See Fig. 5 and 6 for location. a) Cross-section through Niquizanga area. Two faults are mapped and dip about 40°E, with Neogene sediments between them. The faults are parallel to the inherited foliation in the basement. b) Cross-section through Ampacama area. 3 main thrusts are represented with dips about 30° E. Along one of the fault, the fault plane is parallel to the basement foliation, while in the other places it is strongly oblique. Between the basement thrust, the Neogene sediments mainly dip about 30° East. A fourth fault is suspected in the western part, but no Tertiary sediments crop out to confirm it.

Figure 8: Field photographs of folds affecting the basement rocks. The folds display very brittle style with a) kink geometries (site 2, Fig. 5), b) and c) sharp, fractured hinges with

planar limbs (site 10 and 17, respectively, Fig. 5), while the inherited ductile deformation can still be observed as boudins (c). Note that the fold axes are approximately N-S and that preferential vergence of the folds is systematically a West-vergence.

Figure 9: Field photographs of folds affecting the basement rocks. a) Fold with sharp and fractured hinge and b) associated foliation-parallel slip (site 2, Fig. 5). Fold and slip indicate an E-W shortening. c) Larger-scale fold in the basement. Note the W-verging kinematics.

Figure 10: Foliation parallel breccias. a) With no cement (site 23, Fig. 5). b) and c) With more cement (site 10, Fig. 5).

Figure 11: Microphotographs. a) Micaschist (site 4, Fig. 5) with foliation underlined by quartz and micas. b) Quartzo-feldspathic rocks with a high amount of chlorite and no clear anisotropy (site 96, Fig. 6). c) and d) Breccias and calcitic cement in the brecciated layers (site 23, Fig. 5).

Figure 12: Conceptual model of shear zone development. a) Inherited metamorphic foliation with both quartzo-feldspathic and mica-rich layers. b) Shearing induces disharmony with folding of thin quartzo-feldspathic layers embedded between mica-rich layers that most likely accommodate foliation parallel shear. Layer-parallel shortening of the upper quartzo-feldpsathic layer is represented for balancing purposes although this has not clearly been observed in the field. C) Breccias resulting from the breakdown of the folded quartzo-feldspathic layer. The shearing localizes in this

brecciated zone. D) Ultimately, this brecciated layer may evolve as a new local decollement allowing the development of larger folds affecting the upper quartzo-feldspathic layers.

Figure 13: a) Cross section of the Pie de Palo (See Fig. 3 for location) and b) its restoration. In a) the foliation traces are from field observation and geological maps (see Fig. 3) for the surface ones. East of Pie de Palo, at depth, the inherited foliation is projected southward from seismic lines located north-east of Pie de Palo (Zapata, 1998). Seismic foci in the northern part of the Pie de Palo (Regnier et al., 1992) were projected on the section (dots). Pal. for Paleozoic; Neog. for Neogene.

Figure 14: Crustal scale cross-section of both the Sierra Pie de Palo, the Sierra Valle Fertil, and the Precordillera (see Fig. 1B for location). (A) From Verges et al. (2007) and adapted from Verges et al. (2007) (B) in Siame et al. (2015) and (C) this study. In (C), the front of the Precordillera has been modified after Alonso et al. (2014). The asterisk near the star along the western crustal E-verging thrust represents an alternative solution for the 1944 focus (from Meigs and Nabelek, 2010). The 1977M earthquake foci has been translated 30 km to the West as suggested in Regnier et al. (1992).

Figure 15: Lithospheric scale section of the Andes modified from Cristallini and Ramos (2000) (see Fig. 1A for location). The crustal structure at Pie de Palo and below the Precordillera were modified according to the present study. The Moho and lower crustal structure (eclogitized root) are from Ammirati et al. (2013, 2015). The Eastern Sierras Pampeanas structure is from Ramos et al. (2002) and Perarnau et al. (2012).

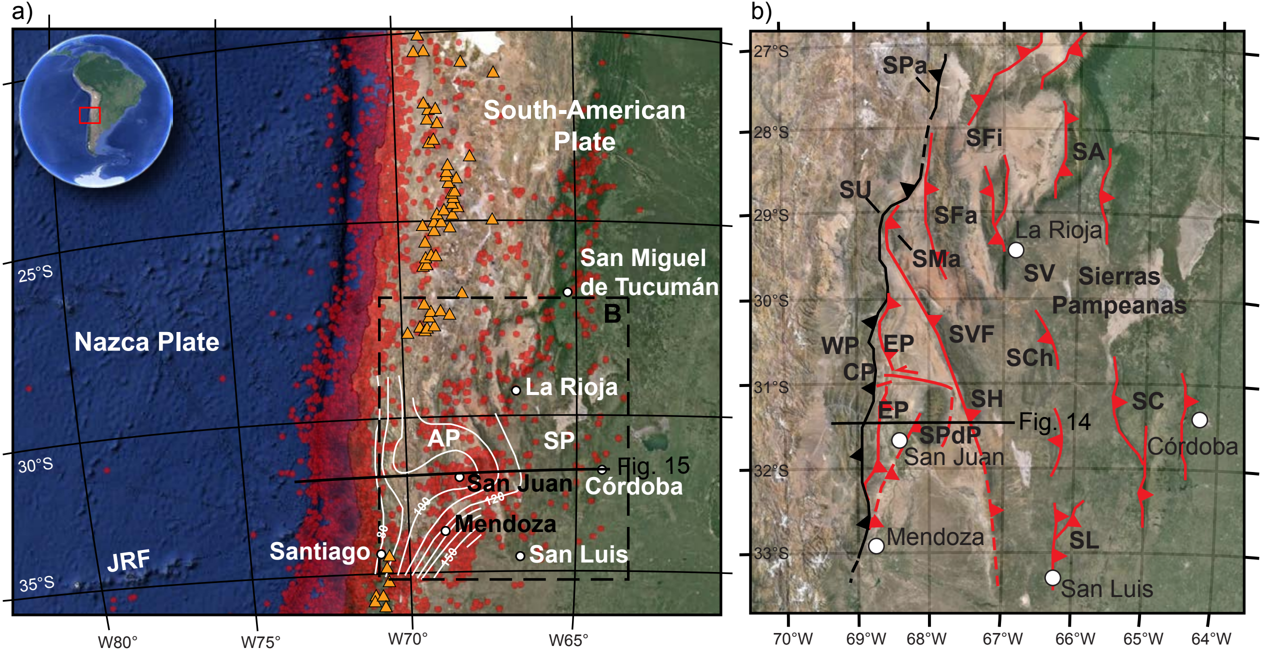
a)
South-American Plate
San Miguel de Tucumán
Nazca Plate
La Rioja
AP
SP
B
San Juan
Córdoba
Fig. 15
Mendoza
Santiago
San Luis
JRF
25°S
30°S
35°S
W80°
W75°
W70°
W65°
80
100
120
150
b)
27°S
28°S
29°S
30°S
31°S
32°S
33°S
SPa
SFi
SA
SU
SFa
La Rioja
SMa
SV
Sierras Pampeanas
WP
EP
SVF
SCh
CP
SH
SC
EP
Fig. 14
SPdP
San Juan
Córdoba
SL
Mendoza
San Luis
70°W
69°W
68°W
67°W
66°W
65°W
64°W

Figure 1

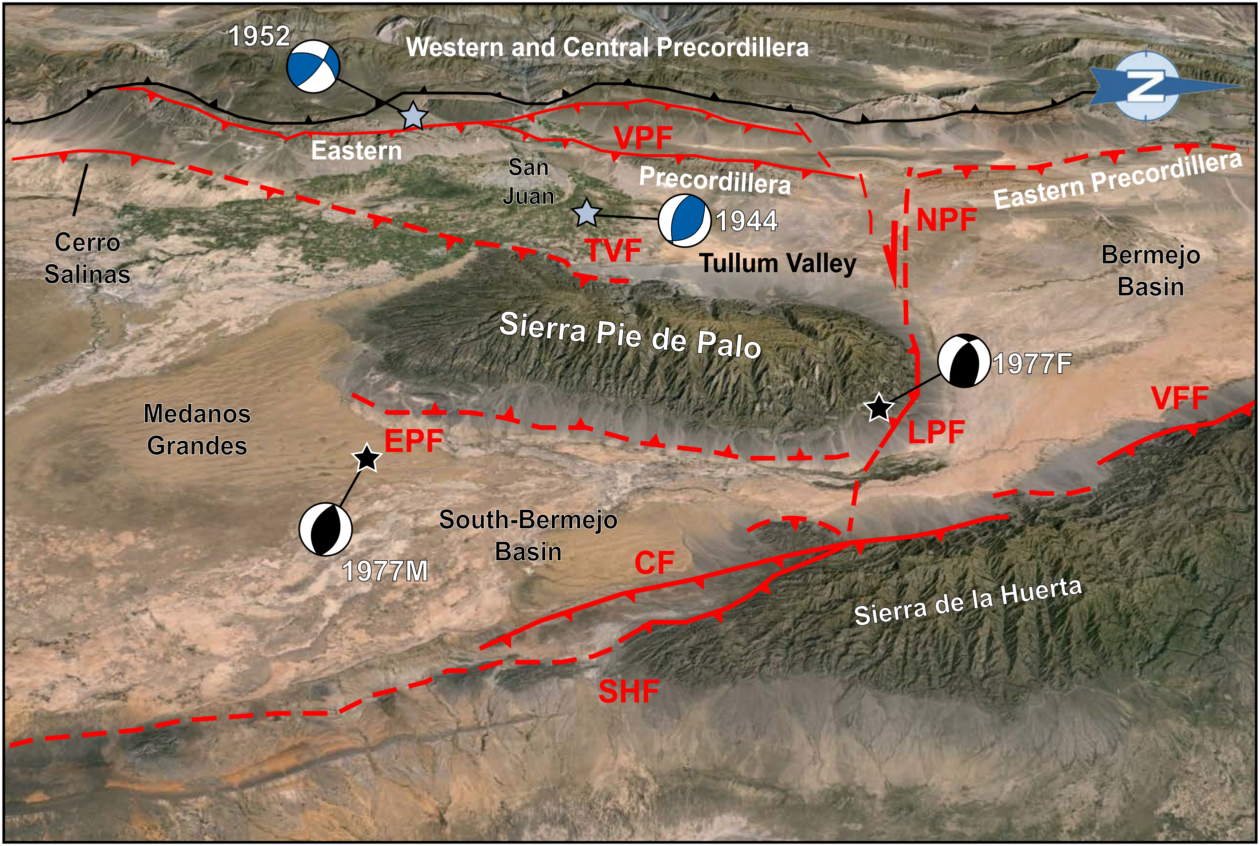

1952
Western and Central Precordillera
Eastern
VPF
San
Juan
Precordillera
Eastern Precordillera
Cerro
Salinas
1944
NPF
TVF
Tullum Valley
Bermejo
Basin
Sierra Pie de Palo
1977F
VFF
Medanos
Grandes
EPF
LPF
South-Bermejo
Basin
1977M
CF
Sierra de la Huerta
SHF

Figure 2

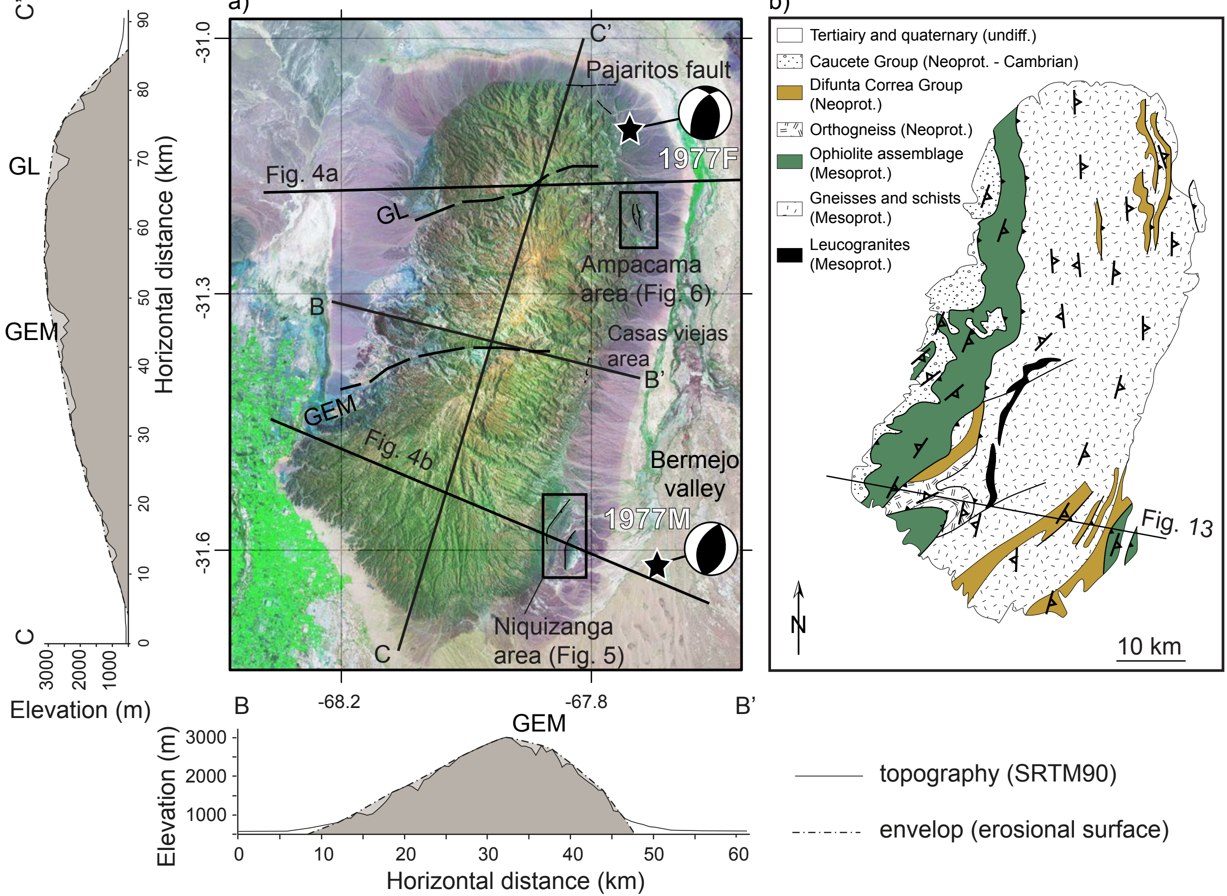

a)
b)
C'
C
GL
GEM
Horizontal distance (km)
Elevation (m)
-31.0
-31.3
-31.6
-68.2
-67.8
Pajaritos fault
1977F
Fig. 4a
Ampacama area (Fig. 6)
B
B'
Casas viejas area
Fig. 4b
Bermejo valley
1977M
Niquizanga area (Fig. 5)
Tertiairy and quaternary (undiff.)
Caucete Group (Neoprot. - Cambrian)
Difunta Correa Group (Neoprot.)
Orthogneiss (Neoprot.)
Ophiolite assemblage (Mesoprot.)
Gneisses and schists (Mesoprot.)
Leucogranites (Mesoprot.)
Fig. 13
N
10 km
topography (SRTM90)
envelop (erosional surface)

Figure 3

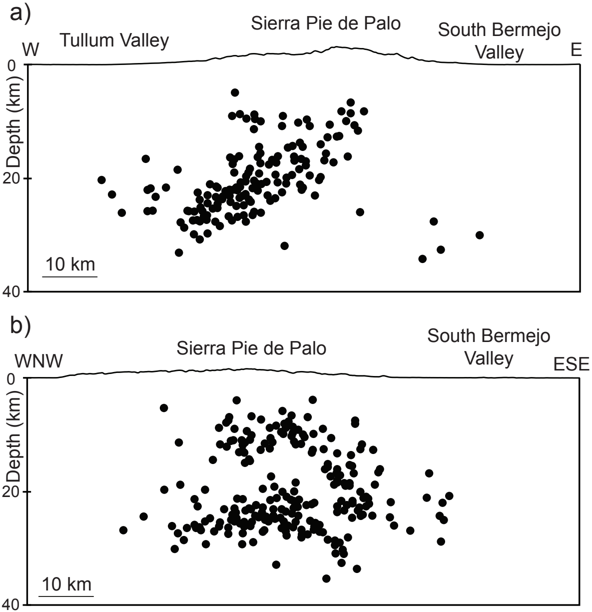
a)
Tullum Valley
Sierra Pie de Palo
South Bermejo Valley
W
E
0
20
40
Depth (km)
10 km
b)
Sierra Pie de Palo
South Bermejo Valley
WNW
ESE
0
20
40
Depth (km)
10 km

Figure 4

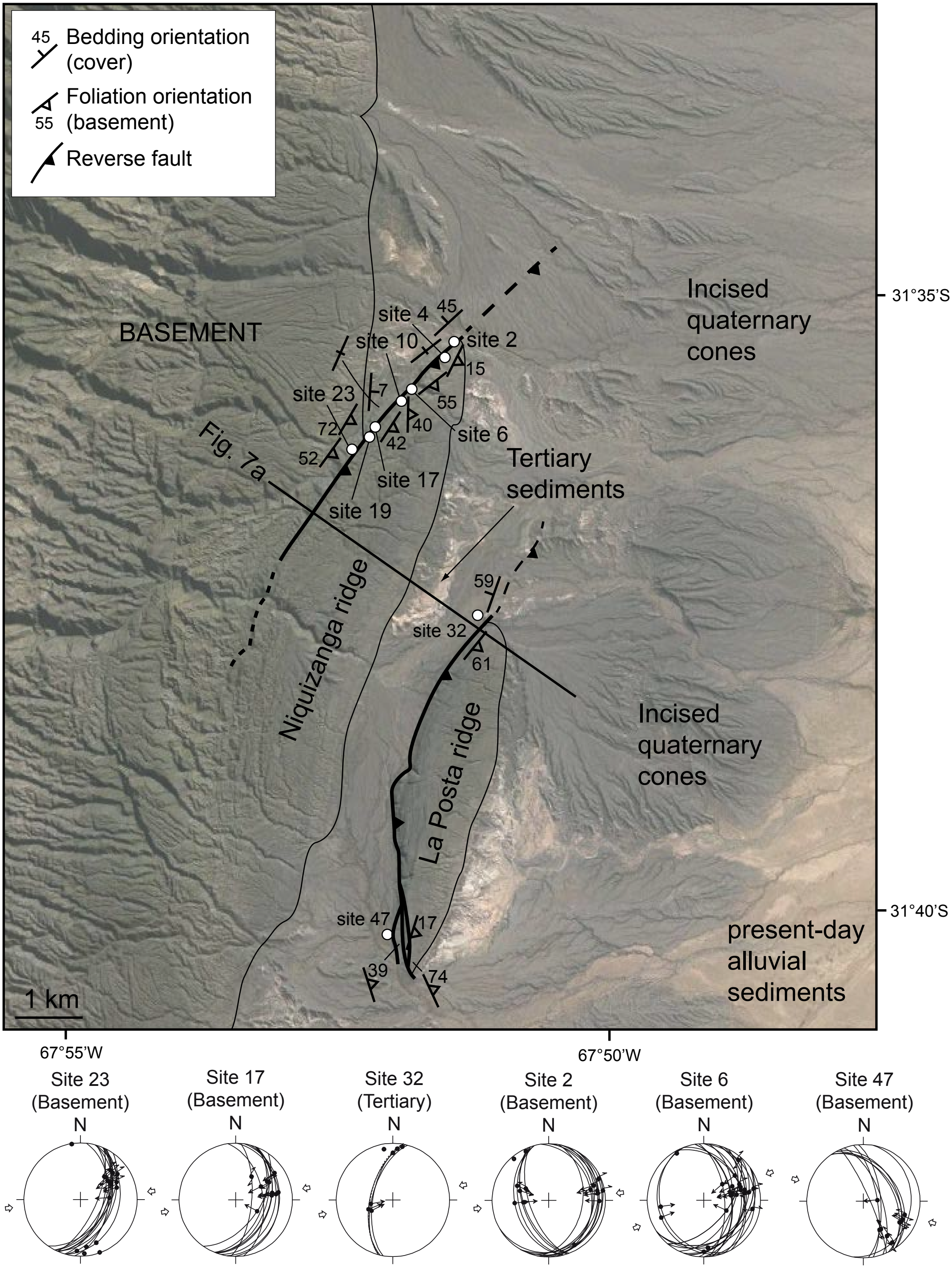
45 Bedding orientation (cover)
Foliation orientation 55 (basement)
Reverse fault
BASEMENT
Incised quaternary cones
Tertiary sediments
present-day alluvial sediments
Niquizanga ridge
La Posta ridge
Fig. 7a
site 2
site 4
site 6
site 10
site 17
site 19
site 23
site 32
site 47
1 km
31°35'S
31°40'S
67°55'W
67°50'W
Site 23 (Basement)
Site 17 (Basement)
Site 32 (Tertiary)
Site 2 (Basement)
Site 6 (Basement)
Site 47 (Basement)
N

Figure 5

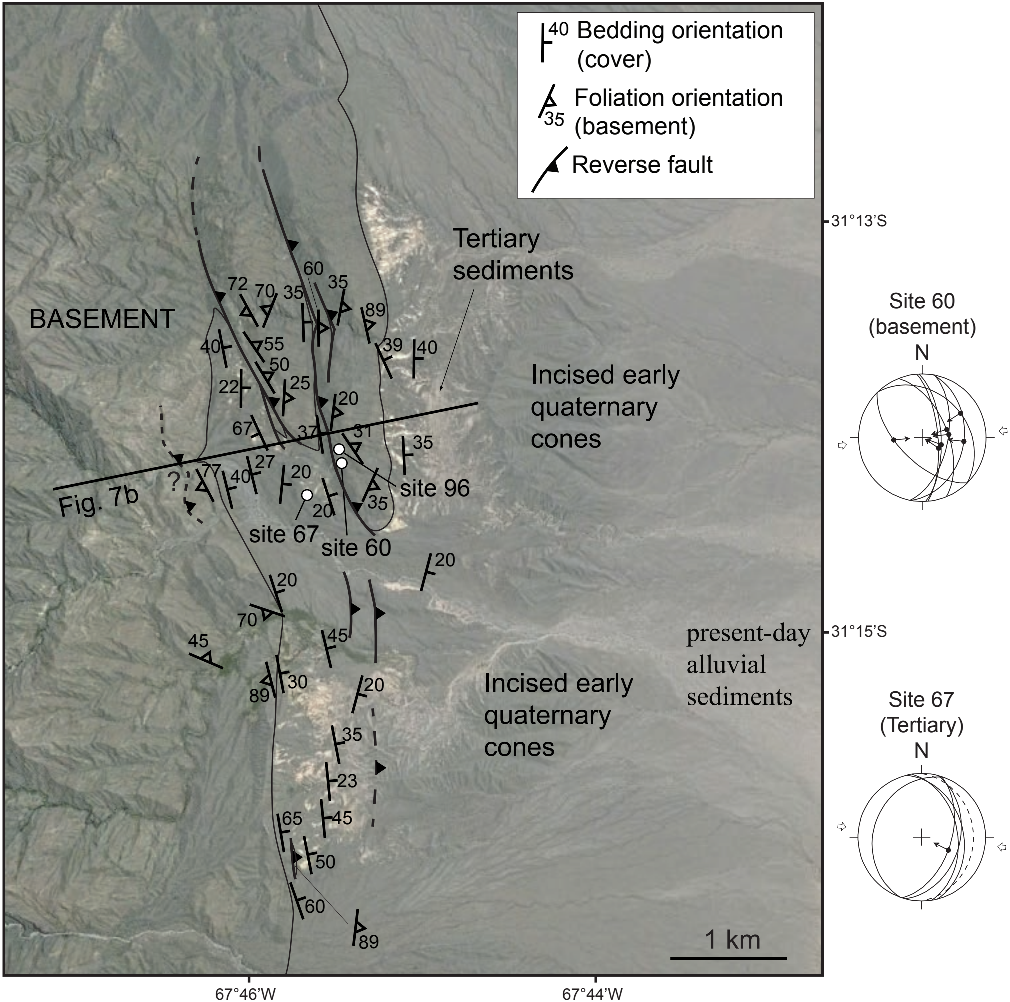

Bedding orientation (cover)
Foliation orientation (basement)
Reverse fault
BASEMENT
Tertiary sediments
Incised early quaternary cones
Fig. 7b
site 96
site 67
site 60
Incised early quaternary cones
present-day alluvial sediments
1 km
31°13'S
31°15'S
67°46'W
67°44'W
Site 60 (basement)
N
Site 67 (Tertiary)
N

Figure 6

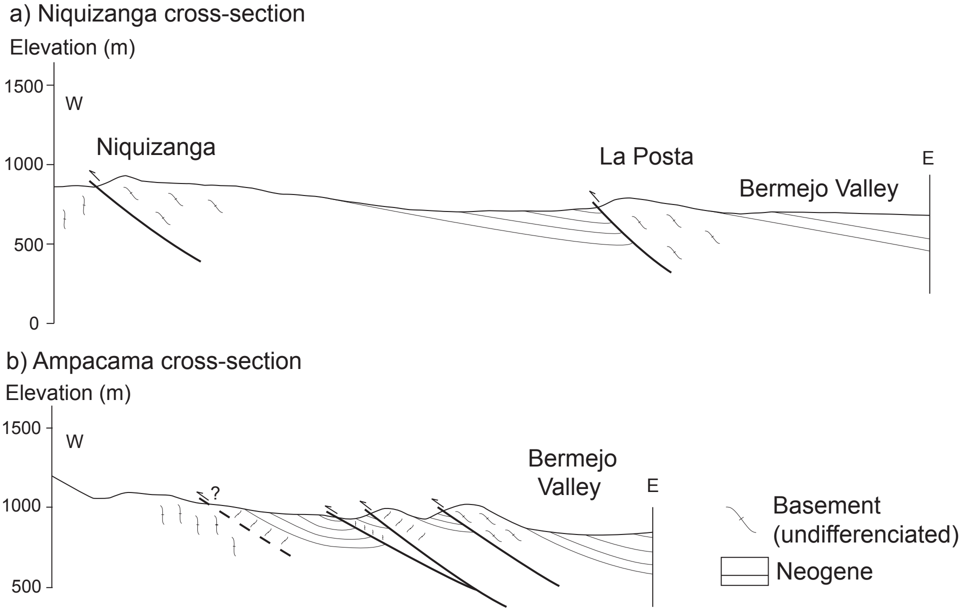
a) Niquizanga cross-section
Elevation (m)
1500
1000
500
0
W
Niquizanga
La Posta
E
Bermejo Valley
b) Ampacama cross-section
Elevation (m)
1500
1000
500
W
?
Bermejo
Valley
E
Basement
(undifferenciated)
Neogene

Figure 7

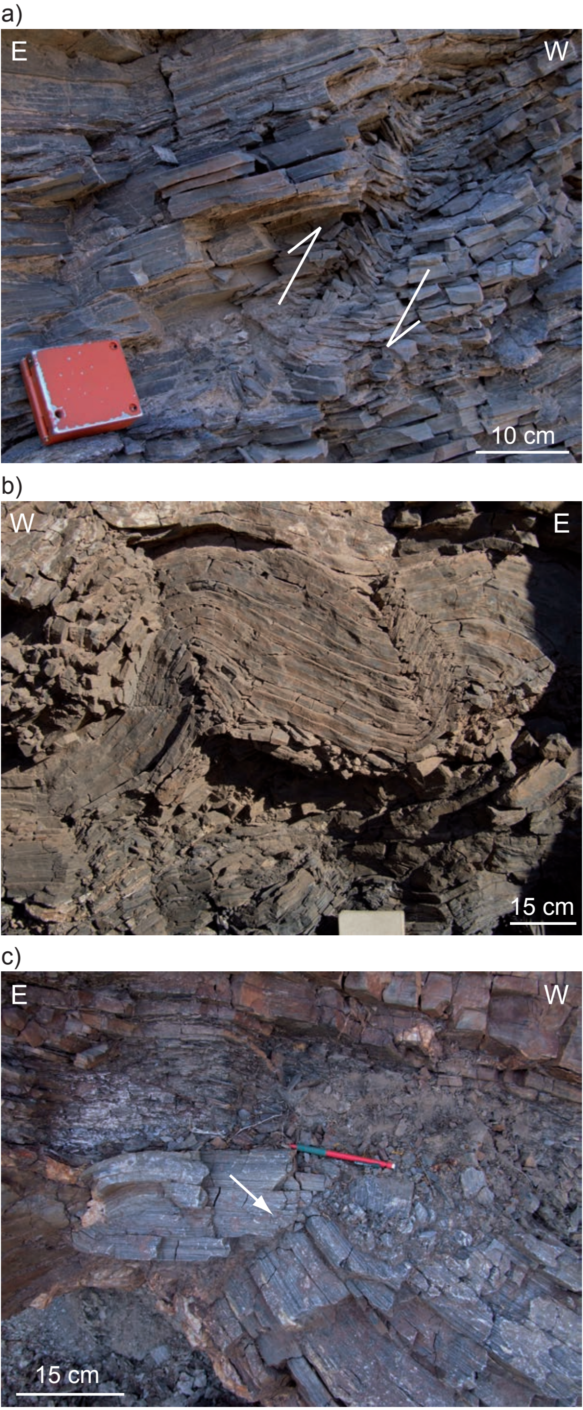

Figure 8

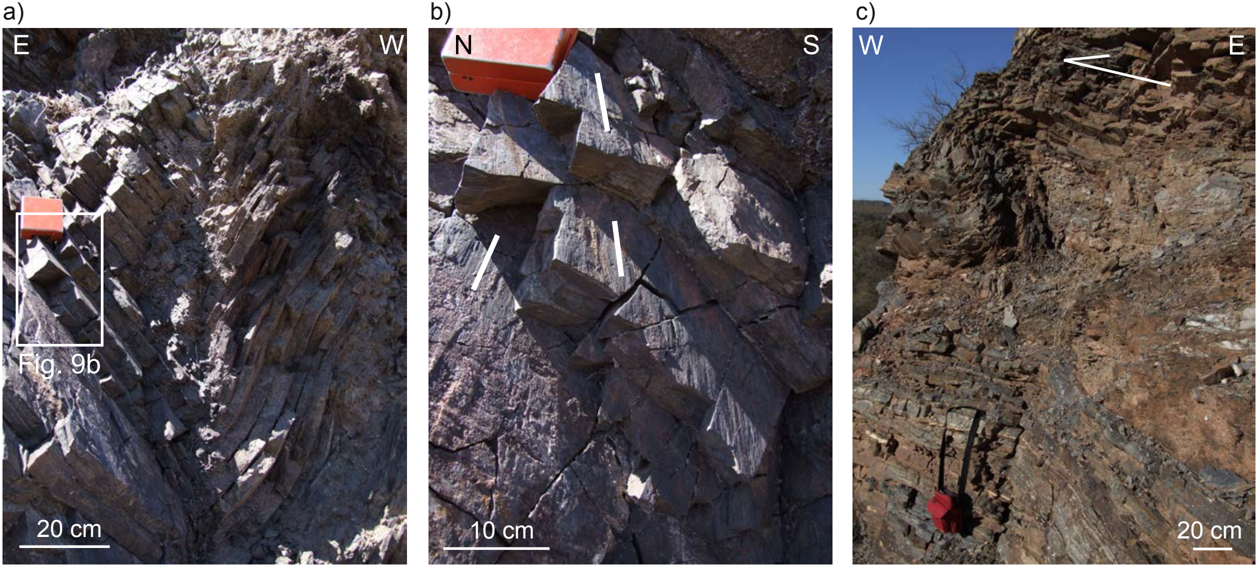

Figure 9

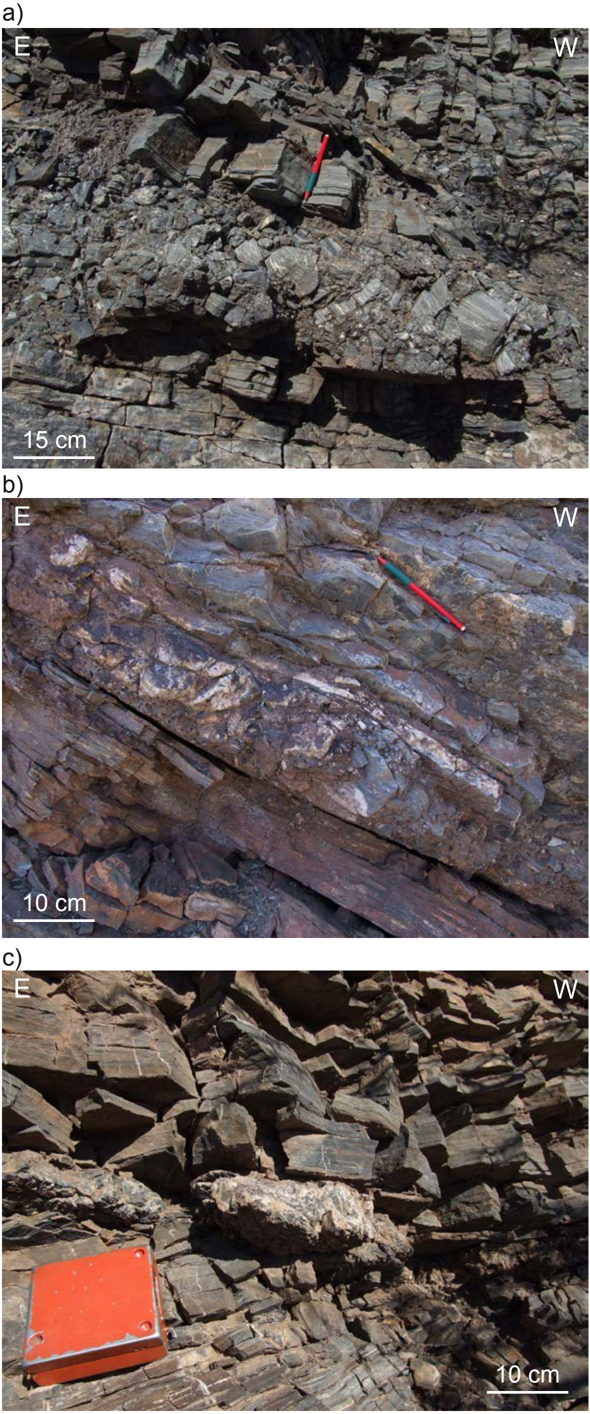

Figure 10

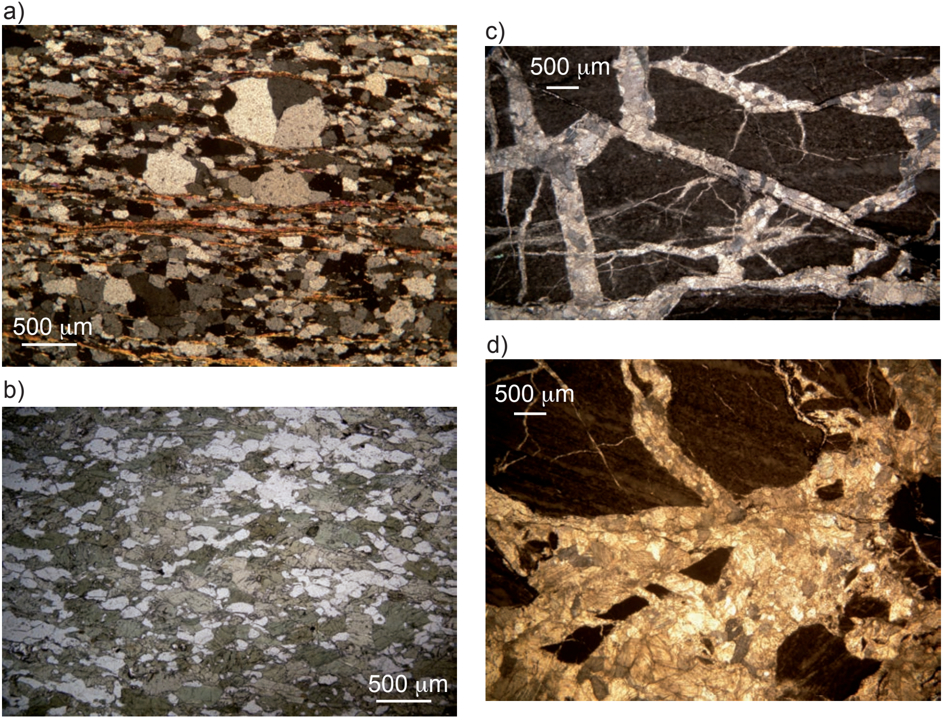

Figure 11

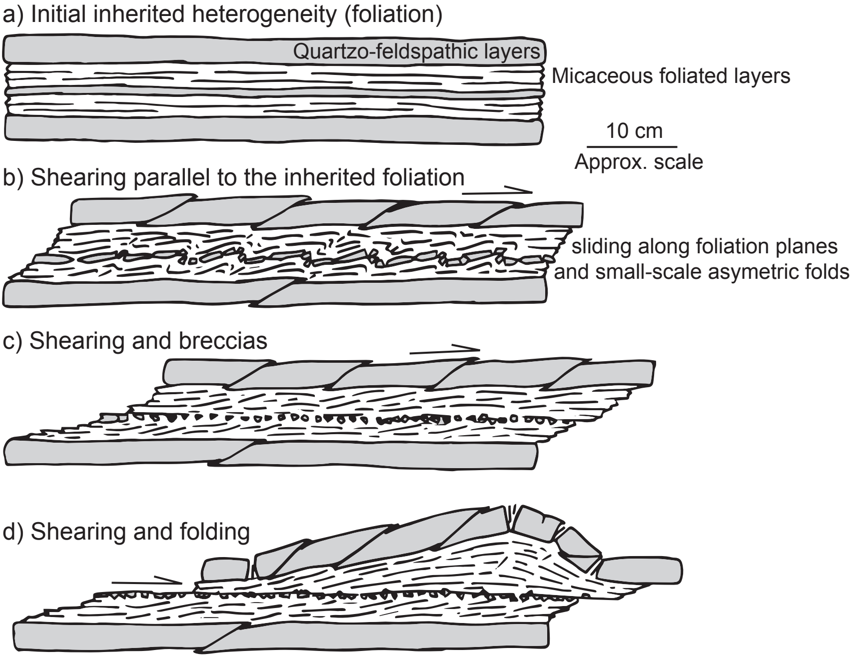
a) Initial inherited heterogeneity (foliation)
Quartzo-feldspathic layers
Micaceous foliated layers
10 cm
Approx. scale
b) Shearing parallel to the inherited foliation
sliding along foliation planes
and small-scale asymetric folds
c) Shearing and breccias
d) Shearing and folding

Figure 12

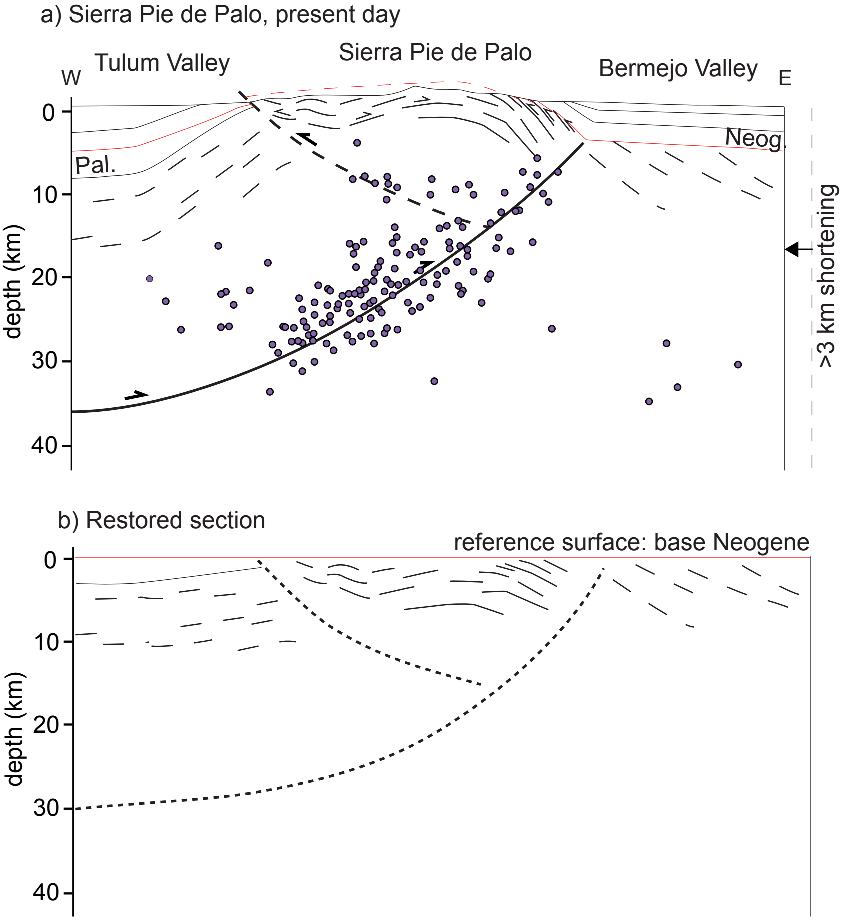
a) Sierra Pie de Palo, present day
W
Tulum Valley
Sierra Pie de Palo
Bermejo Valley
E
0
10
20
30
40
depth (km)
Pal.
Neog.
>3 km shortening
b) Restored section
reference surface: base Neogene
0
10
20
30
40
depth (km)

Figure 13

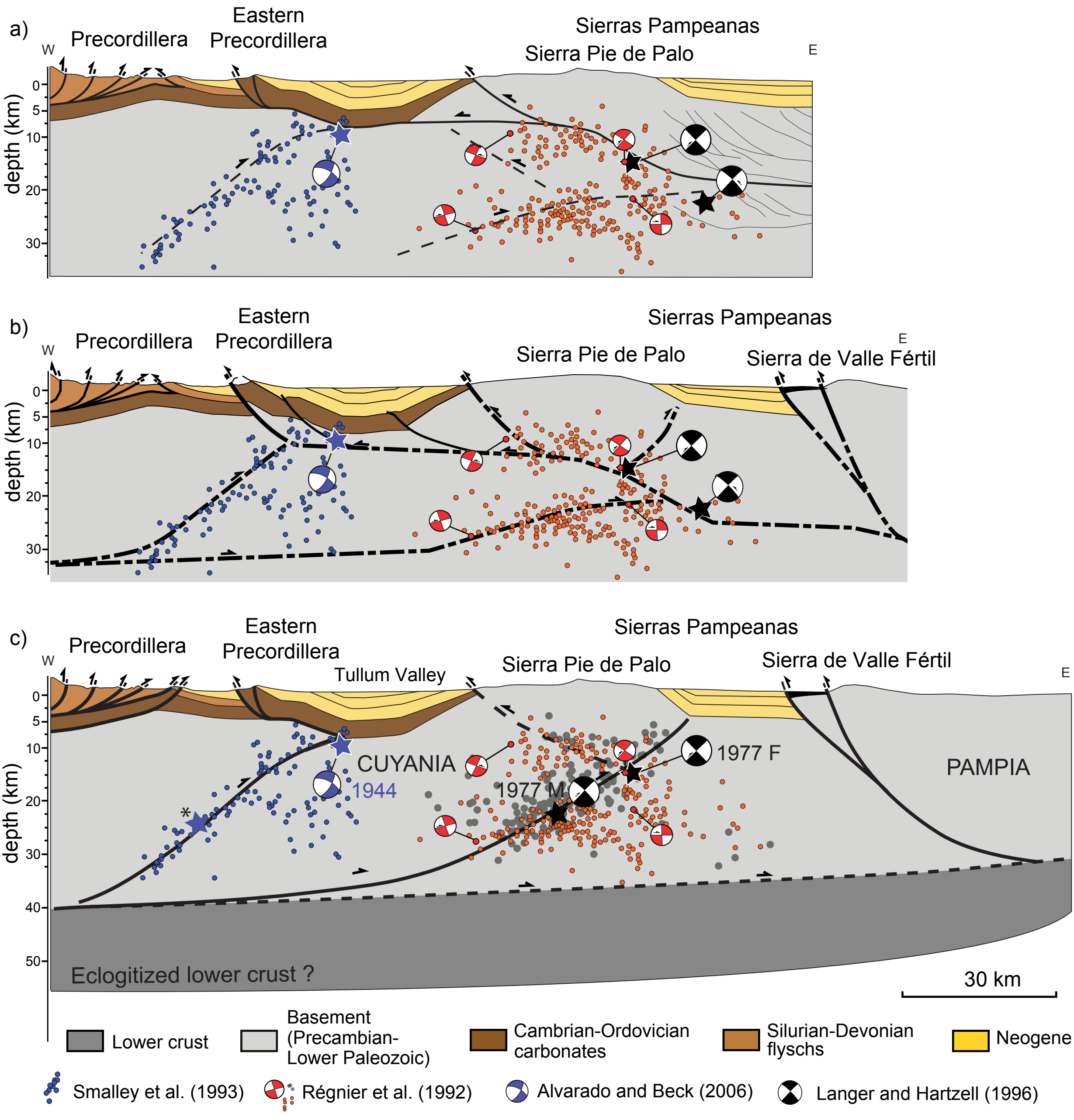
a)
b)
c)
W
E
Precordillera
Eastern Precordillera
Sierras Pampeanas
Sierra Pie de Palo
Sierra de Valle Fértil
Tullum Valley
depth (km)
CUYANIA
PAMPIA
1944
1977 F
1977 M
Eclogitized lower crust ?
30 km
Lower crust
Basement (Precambian-Lower Paleozoic)
Cambrian-Ordovician carbonates
Silurian-Devonian flyschs
Neogene
Smalley et al. (1993)
Régnier et al. (1992)
Alvarado and Beck (2006)
Langer and Hartzell (1996)

Figure 14

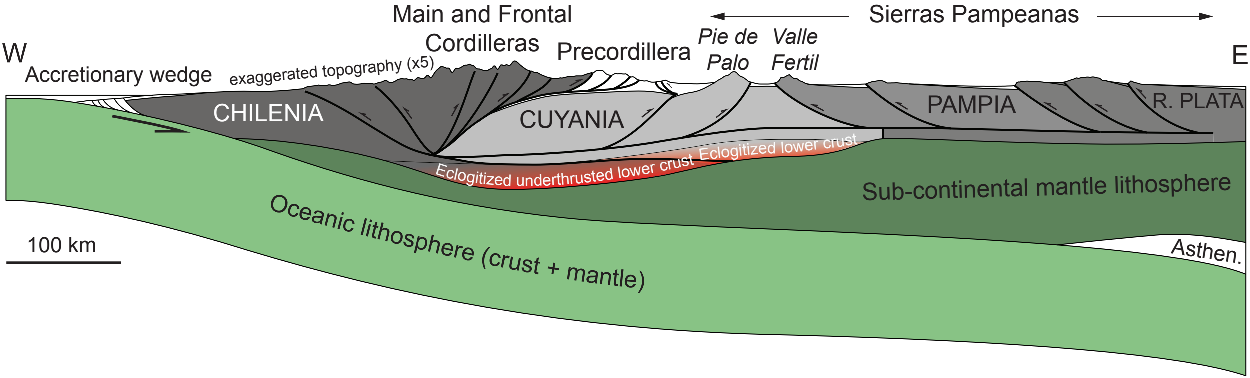
Main and Frontal Cordilleras
Sierras Pampeanas
W
E
Accretionary wedge
exaggerated topography (x5)
Precordillera
Pie de Palo
Valle Fertil
CHILENIA
CUYANIA
PAMPIA
R. PLATA
Eclogitized underthrusted lower crust
Eclogitized lower crust
Sub-continental mantle lithosphere
Oceanic lithosphere (crust + mantle)
100 km
Asthen.

Figure 15